Invasion speeds of *Triatoma dimidiata*, vector of Chagas disease: An application of orthogonal polynomials method

Mohammed Mesk [a,*], Tewfik Mahdjoub [a], Sébastien Gourbière [b], Jorge E. Rabinovich [c], Frédéric Menu [d]

[a] Laboratoire d'Analyse Non Linéaire et Mathématiques Appliquées, Université de Tlemcen, BP 119 Imama (Pôle2), Tlemcen 13000, Algeria
[b] Université de Perpignan Via Domitia, EA 4218 'Institut de Modélisation et d'Analyse en Géo-Environnements et Santé' (IMAGES), Perpignan 66100, France
[c] Centro de Estudios Parasitológicos y de Vectores, Universidad Nacional de La Plata, La Plata, Provincia de Buenos Aires, Argentina
[d] Laboratoire de Biométrie et Biologie Evolutive (UMR 5558), Université de Lyon, Université Lyon 1, UMR CNRS 5558, 43 Bd du 11 Novembre 1918, 69 622 Villeurbanne Cedex, France

HIGHLIGHTS

- A structured integrodifference equation is used to study invasion speed of *T. dimidiata*.
- Importance of seasonal dispersal when estimating the invasion capacity of triatomines.
- An efficient control may be to disturb the transition from juvenile to adult stage.

ARTICLE INFO

ABSTRACT

Demographic processes and spatial dispersal of *Triatoma dimidiata*, a triatomine species vector of Chagas disease, are modeled by integrodifference equations to estimate invasion capacity of this species under different ecological conditions. The application of the theory of orthogonal polynomials and the steepest descent method applied to these equations, allow a good approximation of the abundance of the adult female population and the invasion speed. We show that: (1) under the same mean conditions of demography and dispersal, periodic spatial dispersal results in an invasion speed 2.5 times larger than the invasion speed when spatial dispersal is continuous; (2) when the invasion speed of periodic spatial dispersal is correlated to adverse demographic conditions, it is 34.7% higher as compared to a periodic dispersal that is correlated to good demographic conditions. From our results we conclude, in terms of triatomine population control, that the invasive success of *T. dimidiata* may be most sensitive to the probability of transition from juvenile to adult stage. We discuss our main theoretical predictions in the light of observed data in different triatomines species found in the literature.

1. Introduction

Chagas disease, also known as American trypanosomiasis, is a life-threatening illness caused by the protozoan parasite, *Trypanosoma cruzi*. The disease is endemic in Latin America where *T. cruzi* is primarily transmitted by blood-sucking triatomine bugs (Gourbière et al., 2012), and is now spreading outside of its ancestral geographic range because of increasing international exchanges (Pinto Dias, 2013; Tanowitz et al., 2011).

As an efficient vaccine is still lacking and as it is difficult to deliver medicinal drugs in time (during and shortly after the acute stage of the disease) vector control and blood screening are the main strategies to control the transmission of this disease. Despite the important successes of the national and international control programs launched in the 90s (Abad-Franch et al., 2013), neither the 2005 target of interruption of the transmission of the disease set by the World Health Assembly in 1998, nor the 2010 target for elimination were met (Gürtler et al., 2008).

The evolution of disease transmission indeed lead to new challenges, which currently include the emergence of Chagas disease in regions previously considered to be free of the disease,

* Corresponding author.
  E-mail addresses: m_mesk@mail.univ-tlemcen.dz (M. Mesk),
  tew.mahdjoub@mail.univ-tlemcen.dz (T. Mahdjoub),
  gourbiere@univ-perp.fr (S. Gourbière),
  Jorge.Rabinovich@gmail.com (J.E. Rabinovich),
  frederic.menu@univ-lyon1.fr (F. Menu).

such as the Amazon basin (WHO, 2010), the re-emergence of the disease in regions where control of key domiciliated species, such as *Triatoma infestans*, had been achieved (Gurevitz et al., 2012; Gürtler et al., 2009), and the increasing awareness that non-domiciliated species, such as *T. dimidiata* (Gourbière et al., 2008; Nouvellet et al., 2011) or *Rhodnius prolixus* (Guhl et al., 2009; Hashimoto and Schofield, 2012) can contribute to substantial levels of infection prevalence in humans (Nouvellet et al., 2013; Rascalou et al., 2012).

To deal with such challenges requires a good understanding of the triatomines' demographic and dispersal potentials, and their response to the ongoing environmental changes. The dispersal of triatomines appears as one of the less documented traits, although the ones influencing the rate of flight initiation and its direction have been investigated in the past (Galvão et al., 2001; Minoli and Lazzari, 2006; Pacheco-Tucuch et al., 2012; Schofield et al., 1991), and dispersal distances have recently been estimated more accurately by combining data on insects' spatial distribution and spatial modeling in *T. dimidiata* (Nouvellet et al., 2015). Still, some of the relationships between the demographic/dispersal life-history traits and the invasion capacity of vectors that are spreading into new geographic areas and/or the speed at which they do so, remains to be quantified.

To establish such a quantitative link requires a stage structured spatial modeling to account for the demographic and dispersal specificities of pre-adult and adult triatomines. Spatially explicit models (Dunning Jr. et al., 1995) can be used in this context in view of the geographic nature of the spread of triatomines, see (Nouvellet et al., 2015) for a review on these models and other mathematical models of Chagas disease. The geographic habitat can be modeled in a discrete or in a continuous way. Some common discrete spatio-temporal models as cellular automata (Cissé et al., 2016; Crawford et al., 2013; Slimi et al., 2009), grid-based models (Barbu et al., 2010) and based agent models (Devillers et al., 2008; Yong et al., 2015) have been used to study triatomine or *T. cruzi* invasion of domestic (e.g., (Barbu et al., 2011; Slimi et al., 2009)) and sylvatic areas (Crawford et al., 2013). Examples of spatially explicit continuous models which have been widely used to study the spread of populations and epidemics are based on reaction-diffusion (Petrovskii and Li, 2006; Skellam, 1951), integrodifferential (Medlock and Kot, 2003; Mollison, 1977) and integrodifference (Kot and Schaffer, 1986; Shigesada and Kawasaki, 2002) equations.

The work of Crawford et al. (2013) seems to be the only published work treating invasion speed of Chagas disease. In biological models, the term "invasion speed" (see Appendix A.6 for definition) is generally associated with the speed at which a certain population or infection expands over space. In (Crawford et al., 2013) a two dimentional deterministic cellular automaton (CA) model in the form of a dynamical system with 9376 equations is developed in order to study invasion of a hypothetical strain of *T. cruzi* through the region defined by the primary sylvatic cycles in northern Mexico and parts of the southeastern United States. Hosts are racoons and woodrats which are assumed not to disperse. Vectors are *Triatoma gerstaeckeri* and *T. sanguisuga* which are assumed to disperse during a maximum of 5 weeks. In this (CA) model, the invasion speed of the epidemic has been defined using two distinct methods and examined under different vector migration scenarios.

In this study we use for our modeling a structured integrodifference equation (SIDE) which offers an ideal mathematical framework to model invasions of populations in a constant (Li et al., 2005; Lui, 1989; Neubert and Caswell, 2000), and periodic or stochastic environment (Caswell et al., 2011; Schreiber and Ryan, 2011). Interestingly, under some assumptions (relying on the so called the linear conjecture), the rate of invasion of a nonlinear

SIDE is approached by the rate of invasion of the linear SIDE obtained from the nonlinear SIDE at low densities and is given by an explicit formula (Caswell et al., 2011; Neubert et al., 2000; Schreiber and Ryan, 2011). This formula can also be obtained for a linear SIDE by using an approximation method, called the saddle point (or the steepest descent) method (Radcliffe and Rass, 1997). The saddle-point method is a method used to approximate some specific integrals depending on one parameter when this parameter is large (Murray, 1984). Recently, it was used in (Kot and Neubert, 2008) to analyze the linear unstructured integrodifference equation (UIDE) that models the growth and spread of populations released at the origin in one and two dimensional space: formal solutions were written to the model using the exponential transform and, by the steepest descent method, the asymptotic approximation to the solutions for long times was determined. Moreover, from this approximation, they derived a pair of equations of the rate of invasion which are equivalent to the earlier formulation given by Weinberger (1982). Kot and Neubert (2008) concluded that the saddle-point approximation was excellent not only for long times but also for all times except (possibly) the first few iterations. The steepest descent method has also been applied to infinite-dimensional matrix integrodifference equations (Powell et al., 2005), and used to obtain the speed of propagation for certain continuous time models when the spatial aspect is described by contact distributions (Radcliffe and Rass, 1984). While mathematical expressions of the variation of abundance in space and time have been derived for the linear unstructured case (Kot and Neubert, 2008), such theoretical results remain to be derived for a linearly structured model.

The first aim of this paper is to study the invasion capacity of *T. dimidiata* by calculating its invasion speed and its abundance over time and space in a sylvatic setting by considering different biological situations. We choose this species since data are available in the literature on both its demographic and dispersal parameters (see references above). The dispersal of *T. dimidiata* adults is described by a Laplace kernel in order to account for the long distances traveled by triatomines in their sylvatic biotope (Schofield et al., 1991, 1992).

Our second objective is to propose an original method that relies on orthogonal polynomials to allow calculating both abundances and invasion speed.

We set up a deterministic linear SIDE model with the triatomine population classified in two stages (juveniles and adults) that accounts for their demography and dispersal (in the biological situations considered it is assumed that only adults disperse) in a one dimensional and homogeneous habitat. This model is denoted by 2SIDE. As the density of triatomines and their rates of invasion are important pieces of information, e.g. to manage vector control, we follow here the steps of Kot and Neubert (2008) for the 2SIDE which provides, at the same time, a theoretical extension of the ideas of Kot and Neubert (2008) to a two stages SIDE. This theoretical extension is presented in Appendix A (Section A.3) and it is exemplified by considering two cases: "constant dispersal" and "periodic dispersal". General mathematical results about these two cases are given in Section 2, and detailed analyses are reported in Appendices A and B. The triatomine population densities over time and space can be represented formally by an exponential transform and a specific polynomial set, called orthogonal polynomials which are characterized by a three-term recurrence relation (TTRR) (Chihara, 1978; Szegö, 1975). Then, by the asymptotic behavior of these orthogonal polynomials and the saddle-point method, we determine approximations of the densities for long time periods from which invasion speed formulae can be obtained (see Appendices A and B). The conditions of application to the species *T. dimidiata* are given in Section 3. Specifically, a gradient of biological situations, ranging from the most favorable to the least

favorable demographical conditions are taken into account in estimating the abundance and invasion speeds for both the constant and periodic dispersal cases. In Section 4, we present the results obtained using the available data on the demography and dispersal of *T. dimidiata* to parameterize our model. We took the Laplace dispersal kernel depending on the mean dispersal distance parameter, estimated from previous studies. We calculated the capacity to disperse of triatomines under the two kinds of dispersal described below in Section 2. In each case, the adult density is approximated and their rate of invasion is calculated. We compared saddle-point approximations to exact solutions in the constant case. The end of Section 4 is devoted to sensitivity analysis of the invasion speed to changes in demographic and dispersal parameters. In Section 5, we discuss our main results and give some perspectives to refine this kind of studies.

2. The models

Although the life cycle of triatomines is composed by seven developmental stages: the egg, five larval stages and the adult stage, we considered the development from egg to the fifth larval

$$
\begin{cases}
J_{t+1}(x) = F_{sj}(t)S_j(t)J_t(x) + f_a\left(t, S_{j,1}(t)J_t(x), S_{a,1}(t)\int_{-\infty}^{+\infty} k(x-y)A_t(y)dy\right)S_a(t)\int_{-\infty}^{+\infty} k(x-y)A_t(y)dy \\
A_{t+1}(x) = \left(1 - F_{sj}(t)\right)S_j(t)J_t(x) + S_a(t)\int_{-\infty}^{+\infty} k(x-y)A_t(y)dy
\end{cases}
\tag{1c}
$$

stage as a single stage that we call the juvenile stage as in (Menu et al., 2010).

Assuming a balanced sex ratio, we focused our modeling on the number of female triatomines. During each Δt ($=1$ week) time step, two processes occur: dispersal and demography. We assume that females first disperse to feed (Ceballos et al., 2005; Lehane et al., 1992; Payet et al., 2009; Wisnivesky Colli et al., 1993), making around a single flight per week (Borges et al., 2005; Canals et al., 1999; Catala, 1991), and after reaching their energetic threshold they initiate egg laying (Collier et al., 1977; Friend et al., 1965; Zeledón, 1981). So, we assume that dispersal precedes demography: individuals disperse in $[t, t+\frac{1}{2}]$, and then demography occurs in $[t+\frac{1}{2}, t+1]$. Dividing the interval $[t, t+1]$ into two equal intervals is just a formality: one process can be longer than the other.

The dispersal process is described, in a one-dimensional habitat, by a dispersal kernel $k(|x-y|)$ which represents the probability that an adult moves from location y to location x during one time step. The dependence of the kernel on the distance $|x-y|$ comes from the assumption that the environment is spatially homogeneous.

There is very little information on dispersal with respect to developmental stage. However, the few available data (Forattini et al., 1975; Tonn et al., 1976; Rabinovich, unpublished data) suggest the dispersal of adults is the main factor of triatomine new colony foundation; although 4th and 5th instar nymphs could also participate in the dispersal process (although possibly mainly by human passive dispersal) but 1st, 2nd and 3rd instar nymphs do not disperse, and since in our model we considered only a single juvenile stage, we chose to neglect juvenile dispersal in this paper. The non-dispersal of juveniles is associated with the Dirac delta function $\delta(x-y)$ (Neubert and Caswell, 2000). The densities at time t and location x of the juvenile stage and the adult stage are denoted $J_t(x)$ and $A_t(x)$, respectively.

During a time step, in the interval $[t, t+\frac{1}{2}]$ surviving juveniles with a probability $S_{j,1}(t)$ and dispersing adults which survive with

a probability $S_{a,1}(t)$ are given by

$$
\begin{cases}
J_{t+\frac{1}{2}}(x) = S_{j,1}(t)J_t(x) \\
A_{t+\frac{1}{2}}(x) = S_{a,1}(t)\int_{-\infty}^{+\infty} k(x-y)A_t(y)dy
\end{cases}
\tag{1a}
$$

Then, in the interval $[t+\frac{1}{2}, t+1]$, juveniles surviving with a fraction $S_{j,2}(t)$ may remain in the juvenile stage or develop into the adult stage with probabilities $F_{sj}(t)$ and $F_{ma}(t) = 1 - F_{sj}(t)$, respectively. Adults survive with a probability $S_{a,2}(t)$ and lay eggs with a fecundity density dependent function (number of juveniles/adult during Δt) $f_a\left(t, J_{t+\frac{1}{2}}(x), A_{t+\frac{1}{2}}(x)\right)$. With these notations, mature and reproduction rules can be written

$$
\begin{cases}
J_{t+1}(x) = F_{sj}(t)S_{j,2}(t)J_{t+\frac{1}{2}}(x) + f_a\left(t, J_{t+\frac{1}{2}}(x), A_{t+\frac{1}{2}}(x)\right)S_{a,2}(t)A_{t+\frac{1}{2}}(x) \\
A_{t+1}(x) = \left(1 - F_{sj}(t)\right)S_{j,2}(t)J_{t+\frac{1}{2}}(x) + S_{a,2}(t)A_{t+\frac{1}{2}}(x)
\end{cases}
\tag{1b}
$$

Combining (1a) and (1b) with $S_j(t) = S_{j,1}(t)S_{j,2}(t)$ and $S_a(t) = S_{a,1}(t)S_{a,2}(t)$, the model takes the form of the following integrodifference equations with $J_0(x)$ and $A_0(x)$ known.

Despite the nonlinearity of the fecundity, the broad principle called the "linear conjecture" asserts that the asymptotic invasion speed is determined by the linearization of (1c) at low densities. The linear conjecture is expected to hold provided per capita survivorship and reproduction are greatest at low densities (Mollison, 1991). This conjecture is supported extensively by theory (Lui, 1989; Weinberger, 2002; Weinberger et al., 2002) and numerical simulations (Caswell et al., 2011; Neubert and Caswell, 2000; Neubert et al., 2000; Schreiber and Ryan, 2011).

For the nonlinear model (1c), the linear conjecture applies provided that fecundity is greatest at low densities, i.e. $f_a(t, S_{j,1}(t)J_t(x), S_{a,1}(t)\int_{-\infty}^{+\infty} k(x-y)A_t(y)dy) \leq f_a(t, 0, 0) =: f_a(t)$. Under this condition, and relying on the linear conjecture, the invasion speed is governed by the low-density leading edge of the invasion wave, and the invasion is described by the linear 2SIDE

$$
\begin{cases}
J_{t+1}(x) = F_{sj}(t)S_j(t)J_t(x) + f_a(t)S_a(t)\int_{-\infty}^{+\infty} k(x-y)A_t(y)dy \\
A_{t+1}(x) = \left(1 - F_{sj}(t)\right)S_j(t)J_t(x) + S_a(t)\int_{-\infty}^{+\infty} k(x-y)A_t(y)dy
\end{cases}
\tag{2a}
$$

The demographic and dispersal kernel matrices of the biological model (2a) are given by

$$
\mathbf{B}_t := \begin{pmatrix} b_{11,t} & b_{12,t} \\ b_{21,t} & b_{22,t} \end{pmatrix} = \begin{pmatrix} F_{sj}(t)S_j(t) & f_a(t)S_a(t) \\ \left(1 - F_{sj}(t)\right)S_j(t) & S_a(t) \end{pmatrix}
\tag{2b}
$$
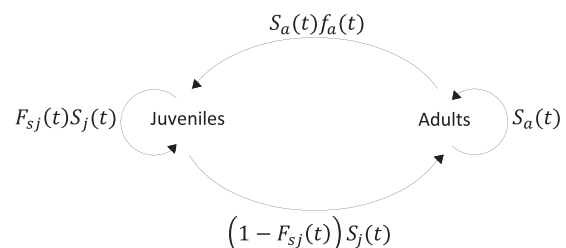
Fig. 1. Schematic representation of the life cycle used in the triatomine model.

and

$$\mathbf{K}(x) := \begin{pmatrix} k_{11}(x) & k_{12}(x) \\ k_{21}(x) & k_{22}(x) \end{pmatrix} = \begin{pmatrix} \delta(x) & k(x) \\ \delta(x) & k(x) \end{pmatrix}, \tag{2c}$$

respectively. For convenience we write $\mathbf{B}_t = (b_{lm,t})$ and $\mathbf{K}(x) = (k_{lm}(x))$, where $l, m \in \{1, 2\}$. The triatomine life cycle used for our modeling is shown in Fig. 1.

With this notation, system (2a) can be written in the following compact form:

$$\boldsymbol{n}_{t+1}(x) = \int_{-\infty}^{+\infty} [\mathbf{K}(x-y) \circ \mathbf{B}_t] \boldsymbol{n}_t(y) dy \tag{3}$$

where $\boldsymbol{n}_t(x) = (J_t(x), A_t(x))'$ and the notations ()$'$ and "$\circ$" indicate the transpose vector and the product term-by-term Hadamard product, of the matrix of dispersal kernels and the projection matrix describing demography, respecively. For the general approach (see Appendix A, Section A.3), the kernels k_{lm} are taken to be time dependent and denoted by $k_{lm,t}$ and the dispersal matrix is also denoted by $\mathbf{K}_t$ or $(k_{lm,t})$.

The existence of solutions of Eq. (3), called traveling waves, was studied both for the scalar (Weinberger, 1982) and structured cases (Caswell et al., 2011; Neubert and Caswell, 2000; Schreiber and Ryan, 2011) considered with or without density dependence. It has been shown, in particular in the latter case, and considering a constant environment ($\mathbf{B}_t \equiv \mathbf{B}$), that when the population initiates its invasion finite in size and restricted to a finite range in space (i.e. the initial conditions have compact support), the waves move along the x-axis position with an invasion speed, given by:

$$\min_{0 < s < \hat{s}} \left[\frac{1}{s} \ln \rho_1(s) \right]. \tag{4}$$

Where $\rho_1(s)$ is the largest eigenvalue of the wave projection matrix $\mathbf{H}(s) = (\hat{h}_{lm}(s)) := \mathbf{B} \circ \hat{\mathbf{K}}(s) = (b_{lm} \hat{k}_{lm}(s))$, with $s \in (0, \hat{s})$ and where $\hat{s}$ is the largest real value for which the $\hat{k}_{lm}(s)$ exist. The elements of the $\hat{\mathbf{K}}(s)$ matrix are the moment generating functions (or the exponential transforms) of the kernels k_{lm}, i.e. $\hat{k}_{lm}(s) = \int_{-\infty}^{+\infty} k_{lm}(x) e^{sx} dx$ for $l, m = 1, 2$ (see Appendix A, Section A.1).

The invasion speed measures the invasive success of the triatomine population. Its value depends implicitly on the population density vector $\boldsymbol{n}_t(x)$. As the expressions of $J_t(x)$ and $A_t(x)$ are coupled (Eq. (2a)), it is sufficient to calculate the population density of adults $A_t(x)$.

The purpose of the next subsections is to calculate the adult density $A_t(x)$ and the invasion speed not only for the case of the 2SIDE in the triatomine's invasion analysis but also for the general demographic matrix $\mathbf{B}_t = (b_{lm,t})$ and the dispersal matrix $\mathbf{K}(x) = (k_{lm}(x))$ cases. Our development of this general analysis is based on the application of orthogonal polynomials and the steepest descent method. We considered two cases; (i) a constant environment, where demographic and dispersal parameters are constant, and which we called the "constant dispersal model"; and (ii) a situation where demographic and dispersal parameters vary with seasons, which we called the "periodic dispersal model". Details of the calculations and demonstrations are reported in Appendix A Section A.4 for the constant model, and Appendix B for the periodic model.

The wave projection matrix $\mathbf{H} = (\hat{h}_{lm})$, its inverse exponential transform $\check{\mathbf{H}} := (h_{lm})$ and the matrix denoted by $\check{\mathbf{H}}_{(r)}$, which was obtained by replacing the second column of $\check{\mathbf{H}}$ by the vector $(J_r \quad A_r)'$, where r, a natural number, play an important role in the results obtained for both the constant and periodic model. Below, we use the trace and determinant notations of a matrix denoted by $tr(\bullet)$ and $det(\bullet)$, respectively. We will also use the notation $det_{cv}(\bullet)$

for the convolution product determinant of a matrix, i.e. $det_{cv}(\check{\mathbf{H}}) = h_{11} * h_{22} - h_{12} * h_{21}$.

2.1. The constant dispersal model

Under a constant environment the projection matrix describing demography takes the form $\mathbf{B}_t = \mathbf{B} = (b_{lm})$ and we have $\mathbf{H} = \mathbf{B} \circ \hat{\mathbf{K}}$ and $\check{\mathbf{H}} = \mathbf{B} \circ \mathbf{K}$.

The exact expression for $A_t(x)$ is then (see Appendix A):

$$A_t = \sum_{l=0}^{\left[\frac{t}{2}\right]} \binom{t-l}{l} (-1)^l \left[A_0 * tr(\check{\mathbf{H}}) - \frac{t-2l}{t-l} det_{cv}(\check{\mathbf{H}}_{(0)}) \right]$$

$$* \left[tr(\check{\mathbf{H}}) \right]^{*(t-1-2l)} * \left[det_{cv}(\check{\mathbf{H}}) \right]^{*(l)} \tag{5}$$

where the variable x is omitted to simplify notation, $\binom{t}{l} = \frac{t!}{l!(t-l)!}$ denotes the binomial coefficients and ()$^{*(n)}$ is the n times convolution product.

An approximation of $A_t(x)$ using the steepest descent method gives:

$$A_t(x) \sim \frac{C(s_0) e^{-x s_0} (\vartheta(s_0))^t}{\sqrt{2\pi |\kappa_1''(s_0)| t}} \tag{6}$$

where $\vartheta(s) = \xi(s) + \sqrt{\xi^2(s) + \eta(s)}$ and $C(s)$ is the function:

$$C(s) = \frac{\hat{A}_1(s) - \hat{A}_0(s) \left(\xi(s) - \sqrt{\xi^2(s) + \eta(s)} \right)}{2\sqrt{\xi^2(s) + \eta(s)}} \tag{7a}$$

depending on $\hat{A}_0(s)$, $\hat{A}_1(s) = b_{21} \hat{k}_{21}(s) \hat{J}_0(s) + b_{22} \hat{k}_{22}(s) \hat{A}_0(s)$, $\xi(s) = \frac{1}{2} tr(\mathbf{H}(s))$ and $\eta(s) = -det(\mathbf{H}(s))$.

To simplify the notations, the natural logarithm of $\vartheta(s)$ is written $\kappa_1(s) = \ln \vartheta(s)$ and is differentiated twice in Eq. (6). All the functions used in formula (6) depend on s_0, root of

$$\frac{\vartheta'(s_0)}{\vartheta(s_0)} = \frac{x}{t}. \tag{7b}$$

The invasion speed, denoted c_{cst}, can then be written (see Appendix A) as

$$c_{cst} = \min_{0 < s < \hat{s}} \frac{1}{s} \ln \vartheta(s). \tag{8}$$

We note that $\vartheta(s)$ is the largest eigenvalue of the wave projection matrix $\mathbf{H}(s)$. It was shown, by a different method in (Neubert and Caswell, 2000), that c_{cst} in formula (8) is an upper bound for the invasion speed of a two stages SIDE with initial conditions having compact support, i.e., they are finite in size and restricted to a finite range in space.

2.2. The periodic dispersal model

A periodic environment can be defined by a set of phases (e.g., seasons), each providing a constant environment. If the number of phases is T, then the environment is called T-periodic. For each phase j ($j = 1, ..., T$), the demographic, the dispersal and the wave projection matrices are respectively $\mathbf{B}_j$, $\mathbf{K}_j$ and $\mathbf{H}_j$.

If r is the time of the census at the beginning of each phase ($r = 0 ... T - 1$) then, after t periods, the density of adults is (see Appendix B):

$$A_{tT+r} = \sum_{l=0}^{\left[\frac{t}{2}\right]} \binom{t-l}{l} (-1)^l \left[A_r * tr(\check{\mathbf{H}}) - \frac{t-2l}{t-l} det_{cv}(\check{\mathbf{H}}_{(r)}) \right]$$

$$* \left[tr(\check{\mathbf{H}}) \right]^{*(t-1-2l)} * \left[det_{cv}(\check{\mathbf{H}}) \right]^{*(l)} \tag{9}$$

where $\mathbf{H}$ is the wave projection matrix over a complete

environmental cycle (from t to $t+T$), given by $\mathbf{H} = \mathbf{H}_T \mathbf{H}_{T-1} \ldots \mathbf{H}_1$ and $\mathbf{H}_j = \mathbf{B}_j \circ \mathbf{\hat{K}}_j$ (Caswell et al., 2011). It should be remembered that $\mathbf{\check{H}}$ is the inverse exponential transform of $\mathbf{H}$.

An approximation of $A_{tT+r}(x)$ can be calculated as in the "constant dispersal model" and gives:

$$A_{tT+r}(x) \sim \frac{C_1(s_0) e^{-xs_0} \big(\vartheta_1(s_0)\big)^t}{\sqrt{2\pi |\kappa''_{11}(s_0)| t}} \tag{10}$$

where $\vartheta_1(s) = \xi_1(s) + \sqrt{\xi_1^2(s) + \eta_1(s)}$ and $C_1(s)$ is the function

$$C_1(s) = \frac{\hat{A}_{T+r}(s) - \hat{A}_r(s)\left(\xi_1(s) - \sqrt{\xi_1^2(s) + \eta_1(s)}\right)}{2\sqrt{\xi_1^2(s) + \eta_1(s)}} \tag{11a}$$

depending on $\hat{A}_r(s)$, $\hat{A}_{T+r}(s) = \hat{h}_{21}(s)\hat{J}_r(s) + \hat{h}_{22}(s)\hat{A}_r(s)$, $\xi_1(s) = \frac{1}{2}tr(\mathbf{H})$ and $\eta_1(s) = -det(\mathbf{H})$.

Here, $\vartheta_1(s)$ is the largest eigenvalue of the wave projection matrix $\mathbf{H}(s)$, $\kappa_{11}(s) = \ln \vartheta_1(s)$ and s_0 is the root of the equation

$$\frac{\vartheta'_1(s_0)}{\vartheta_1(s_0)} = \frac{x}{t}. \tag{11b}$$

The invasion speed, measured as distance per unit time step of T, is then

$$c_{per} = \min_{0 < s < \hat{s}} \frac{1}{S} \ln\big(\vartheta_1(s)\big). \tag{12}$$

For both the constant and periodic models, the relative error $RE_t(x)$ is defined as the difference between the exact value of the abundance and its approximation as given in Eq. (6) (constant model) or in Eq. (10) (periodic model), divided by the exact value.

The aim of the next section is to use these theoretical results to study the invasive capability of the triatomine species *T. dimidiata*.

3. Application to *T. dimidiata*

3.1. The constant case

This case corresponds to a constant spatial dispersal in time. Four sets of demographic parameters are considered according to four environmental settings. They are denoted CD_i where (1) $i = lab$, when demographic parameters are those measured in laboratory experiments; (2) $i = 50\%\ lab$, when demographic parameters are taken to be 50% of their value in the lab; (3) $i = f_{a\_field}$, when the fertility is equal to what has been measured in the field, while the values of other demographic parameters are those measured in the laboratory; and (4) $i = all\_bad$, when demographic parameters are at their minimum value, i.e., a value corresponding to field measurements or 50% of their lab value. These can be

described as high ($i = lab$), moderate ($i = 50\%lab$ or $i = f_{a\_field}$) and weak ($i = all\_bad$) demographic values.

Numerical values of *T. dimidiata's* demographic parameters were obtained from the laboratory (Zeledón, 1981; Zeledón et al., 1970), were calculated for a time step $\Delta t = 1$ week. The average development time from egg to adult is $T_d = 38.05$ weeks. The probability F_{sj} of remaining in the juvenile stage is $F_{sj} = \exp(-1/38.05) = 0.974$. The percentage of juvenile survival is $S = 58.58\%$, so the per unit time probability of survival during the juvenile stage is $0.5858^{\frac{1}{38.05}} = 0.986$. The average lifespan of the adult female is $L = 480$ days or 68.57 weeks, so the per unit time probability of survival of adult females is $S_a = 1 - \frac{1}{68.57} = 0.985$. The average number of eggs/female/life is $F = 605.86$ eggs, and for a balanced sex ratio, $F_f = 303$ female eggs/female/life. So, $f_a = F_f / 68.57 = 4.42$ female eggs/week. The field demographic parameters are fecundity, $f_{a\_field} = 0.434$ female eggs/three months, and adult survival, $S_{a\_field} = 0.223$ in three months (Barbu et al., 2011). Calibrating to one week we find $f_{a\_field} = 0.434/13 = 0.0334$ female eggs/week and $S_{a\_field} = (0.223)^{1/13} = 0.891$.

The values of the demographic parameters corresponding to the four biological situations CD_{lab}, $CD_{50\%lab}$, $CD_{f_{a\_field}}$ and CD_{all_bad} are given in Table 1.

Dispersal of adults is described by the Laplace kernel $k_\alpha(x) = (1/2\alpha)exp(-|x|/\alpha)$, which implies that the probability to disperse decreases with the dispersal distance. The parameter alpha (in meter units) is the mean of the dispersal distance traveled by a sample of adults during the time step. The mean dispersal distances of *T. dimidiata* was estimated from data of year-round travel by Barbu et al. (2010), and in a non-fully sylvatic context, during one time step of two weeks, to be around 40 to 60 m. As in our model the time step is of one week, we considered a field estimate of $\alpha = 30$ m. This choice of α and the Laplace kernel is justified by the fact that in the more realistic case, the periodic case below where $\alpha = 120$ m, the Laplace kernel takes into account the long distances traveled in a single flight by *T. infestans* and *T. sordida* observed under the vector's natural climatic conditions (Schofield et al., 1991, 1992). On average 44% flew farther than 100 m for a single flight (see (Crawford and Kribs-Zaleta, 2013) for a summary) and the Laplace kernel gives for $\alpha = 120$ m approximately the same proportion $\int_{|x| > 100} k_{120}(x)dx = 43.5\%$. That proportion of 44% is for a single flight. As the time step of our model is one week, we assumed (see above) that adults (on average) disperse once in a week. We consider that this mean value of α is not an extremely low value for a sylvatic biotope.

3.2. The periodic case

Seasonality affects demographic and dispersal parameters; according to field studies in the Yucatan peninsula, Mexico, *T. dimidiata* dispersal shows a strong seasonal pattern with a three

Table 1

Values of the demographic parameters for *T. dimidiata* corresponding to the constant dispersal case (CD_i), the period of dispersal (D_i), and non-dispersal (ND_i) in the periodic dispersal case.

Sets of demographic values	f_a (eggs/week), Adult fecundity	S_a (Adult survival probability)	S_j (Juvenile survival probability)	F_{ma} (Transition probability)
CD_{lab}-D_{lab}-ND_{lab}	4.420	0.985	0.986	0.026
$CD_{50\%lab}$ - $D_{50\%lab}$-$ND_{50\%lab}$	2.210	0.492	0.493	0.013
$D_{50\%f_a}$ - $ND_{50\%f_a}$	2.210	0.985	0.986	0.026
$D_{50\%S_a}$ - $ND_{50\%S_a}$	4.420	0.492	0.986	0.026
$D_{50\%S_j}$ - $ND_{50\%S_j}$	4.420	0.985	0.493	0.026
$D_{50\%F_{ma}}$ - $ND_{50\%F_{ma}}$	4.420	0.985	0.986	0.013
$CD_{f_{a\_field}}$-$D_{f_{a\_field}}$-$ND_{f_{a\_field}}$	0.033	0.985	0.986	0.026
$D_{S_{a\_field}}$-$ND_{S_{a\_field}}$	4.420	0.891	0.986	0.026
CD_{all_bad}-D_{all_bad}-ND_{all_bad}	0.033	0.492	0.493	0.013

months period of dispersal from April to June (A–J) that has been consistently observed over the last 10 years (Dumonteil et al., 2013; Dumonteil et al., 2002; Waleckx et al., 2015b). So we considered a Laplace kernel with a dispersal parameter α representing the dispersal capacity in meters as the mean of the dispersal season A–J, and the Dirac delta function for the other seasons with no dispersal. To have the same average dispersal capacity as in the constant case, we considered $\alpha = 120$ m in A–J.

Sets of values of demographic parameters values associated with the period of dispersal or non-dispersal are then denoted D_i and ND_i respectively. In addition to the values of the constant model, five new index values i were defined: (1) $i=50\%f_a$ corresponding to values measured in the lab except for the fertility f_a which was reduced to 50% of its lab value; (2) $i=50\%S_a$ corresponding to laboratory values for all demographic parameters except S_a, which was considered to be 50% of its lab value; (3) $i=50\%S_j$ corresponding to the laboratory values for all parameters except S_j, which was considered to be 50% of the value of the laboratory; (4) $i=50\%F_{ma}$ corresponding to the laboratory values for all parameters except F_{ma}, which was considered to be 50% of the value measured in the laboratory, and (5) $i=S_{a\_field}$ corresponding to laboratory values for all demographic parameters except S_a, which corresponds to a field value (Barbu et al., 2011).

While a constant environment is characterized by a single set of demographic parameters, a periodic environment is described by a pair of demographic sets,

$i, j \in \{$lab, 50%lab, $50\%f_a$, $50\%S_a$, $50\%S_j$, $50\%F_{ma}$, f_{a_field}, S_{a_field}, all_bad$\}$.

The definitions of the different sets of parameters for the periodic case are shown in Table 1.

3.2.1. Different biological situations

Three ecological situations were considered with respect to the environmental conditions encountered during the periods of dispersal and non-dispersal. The first (situation 1), is where the same demographic conditions are considered during periods of dispersal and non-dispersal. The second (situation 2) and third (situation 3) situations, correspond to more realistic conditions. We suppose unfavorable demographic conditions during the period of non-dispersal and favorable demographic conditions during the period of dispersal in situation 2, and favorable demography during the period of non-dispersal and unfavorable demographic conditions for the dispersal period in the situation 3. These two situations correspond to alternative ecological conditions as explained below.

Situation 1. The same demographic parameters are considered during the dispersal and non-dispersal periods. Although this case is likely not to be biologically realistic, it was considered because it is close to the constant case. The abundances $A_t(x)$ and their invasion speed c_{per} are then estimated with the parameter sets , where: (1) $i=j=lab$ (2) $i=j=50\%lab$ and (3) $i=j=all\_bad$.

Situation 2. In situation 2, we assume spatial dispersal induced by a density-dependent mechanism during the period of a favorable demography. Conversely, during the period of unfavorable demography, we assume that no density dependence occurs, as well as no dispersal. This situation corresponds to an unfavorable demography during the sedentary period and a favorable one during the spatial dispersal period. Representative sets of demographic parameters are (D_i, ND_j) where: $i=lab$ and $j = 50\%f_a$, $50\%S_a$, $50\%S_j$, $50\%F_{ma}$, f_{a_field} and S_{a_field}.

Situation 3. In this case, we assume that the spatial dispersal is induced by the depletion of hosts, creating an unfavorable environment that impacts negatively on the demography of

triatomines. Conversely, during the period where hosts are present, the demography is favorable and then triatomines do not disperse. In summary, situation 3 corresponds to favorable demography during the period of non-dispersal and unfavorable demography during dispersal. This situation 3 can also be considered to correspond to occurrence of hurricanes (that is known to result in passive dispersal of triatomines (Guzman-Tapia et al., 2005) that combines both low demography and dispersal. Adult density $A_t(x)$ and invasion speed c_{per} will be estimated with parameters sets (D_i, ND_j) where: $j = lab$ and $i = 50\%f_a$, $50\%S_a$, $50\%S_j$, $50\%F_{ma}$, f_{a_field} and S_{a_field}.

3.2.2. Duration of the dispersal period

The effect of lengthening the duration of the dispersal period was analyzed by assuming that triatomines disperse not only during the season A–J but also during the season July to September (J–S). We then denoted the demographic parameters as $(2D_i, ND_j)$, where i and j belong to the same set as when assuming a single period of dispersal. To maintain an average capacity of dispersal of $\alpha = 30$ m, as in the case of a constant dispersal, α was set to 60 m.

3.2.3. Calculating the invasion speed

Let H_{OD}, H_{JM}, H_{AJ}, H_{JS} be the projection matrices defined for a one week time step during the different seasons O–D, J–M, A–J and J–S respectively. Then H_{OD}^{13}, H_{JM}^{13}, H_{AJ}^{13} and H_{JS}^{13} are the projection matrices of each season and the matrix $H = H_{OD}^{13} H_{JM}^{13} H_{AJ}^{13} H_{JS}^{13}$ is the projection matrix of one year. The invasion speed, measured as distance per a unit time step of one year, is calculated from Eq. (12), namely $c_{per} = \min_{0 < s < \dot{s}} \frac{1}{s} \ln(\vartheta_1(s))$, where $\vartheta_1(s)$ is the dominant eigenvalue of the matrix H.

In the case of a constant dispersal, all projection matrices are equal and the invasion speed can be calculated in the same way.

3.3. Sensitivity analysis

The sensitivity of the invasion speed c_l ($l=cst$ or per) to a parameter θ is given by the derivative of c_l with respect to θ, i.e. $dc_l/d\theta$. With a perturbation $\Delta\theta$ on θ, the sensitivity of c_l can be approximated by $(c_l(\theta+\Delta\theta) - c_l(\theta))/\Delta\theta$, and the elasticity is defined as $(dc_l/c_l)/(d\theta/\theta)$. For a periodic environment of period T, let θ_j be the value of θ during the phase j. Then, the sensitivity (elasticity) of c_l to θ is the mean of the sensitivities (elasticities) of c_l to θ_j, i.e $\left(\sum_{j=1}^{T} dc_l/d\theta_j\right)/T$ and $\left(\sum_{j=1}^{T} (\theta_j/c_l)dc_l/d\theta_j\right)/T$, respectively (Caswell et al., 2011).

4. Results

4.1. Constant dispersal case

Changes in abundance of adults in the case of a constant dispersal with laboratory parameters are shown in Fig. 2. The curves, for weeks 5, 10, 20 and 30, show an increase in the density of adults per point habitat and an increase of the distance dispersed (about 500 m after 30 weeks).

The curves obtained by the approximation in Eq. (6) conform well with those obtained by the exact expression defined in Eq. (5) except near the origin. According to Eq. (6), the relative error between the exact expression and its approximation tends to zero (as t increases, the error curve approaches the x-axis). For instance the graphs represented in Fig. 3 for a chosen situation, show that this error decreases for increasing time.

In the constant dispersal case, when the laboratory demographic parameters are used, the speed of invasion $c_{cst} = 26.80$ m/
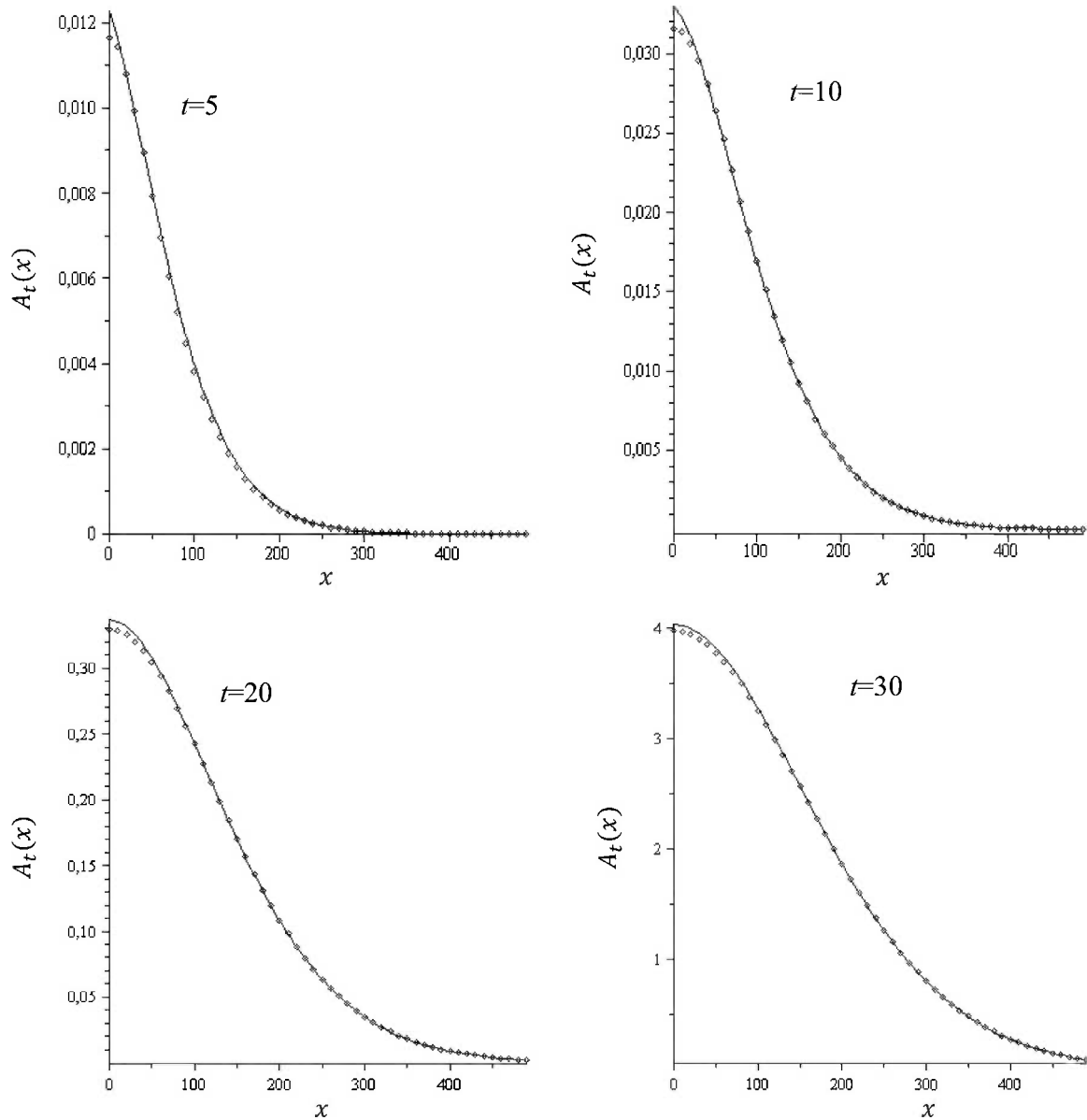
Fig. 2. Plots of the exact solution of Eq. (5) (solid curves) and the approximation in Eq. (6) (dotted curves) for the Laplace distribution with $\alpha = 30$ m, $J_0(x) = 0$ and $A_0(x) = \delta(x)$, the set of demographic parameters CD_{lab} for $t = 5, 10, 20$ and 30 weeks. The x-axis represents the distance (measured from the origin) traveled by adults.
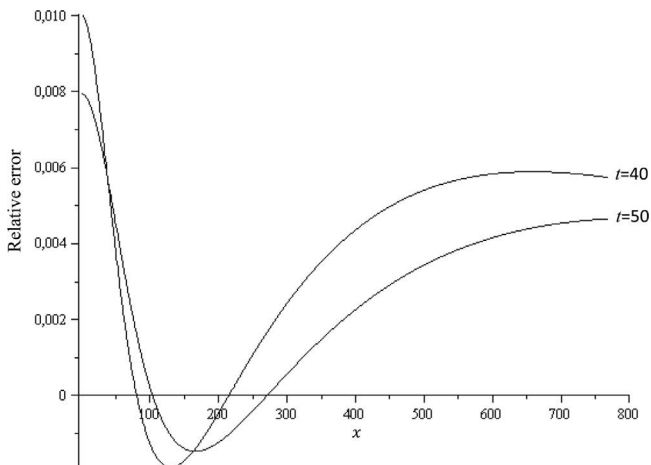
Fig. 3. The relative error between the approximation in Eq. (6) and the exact solution in Eq. (5) as a function of distance x with $\alpha = 10$ m, for $t = 40$ and $t = 50$ in the case of the set of demographic parameters CD_{lab}.

w. This value drops to 3.3 m/w if field fertility is considered (case shown in Fig. 4). For the sets of demographic parameters $CD_{50\%lab}$ and CD_{all_bad}, population extinction is expected. The invasion speed is very sensitive to the probability of transition from juvenile to adult stage. Finally, the elasticity of the invasion speed is larger compared to the survival of adult S_a: in fact, a variation of 1% in S_a causes a variation of 1.5% in the rate of invasion c_{cst}. See Fig. 5 and sensitivity analysis in section 4.3.

4.2. Periodic dispersal case

The distribution of adult densities in the case of a periodic dispersal has the same pattern as the constant case for different equivalent dispersal capacities ($\alpha = 40, 120, 200$ m) and the same couples of sets of the demographic parameters (Figs 6 and 7).

The most important results concern the invasion speeds of *T. dimidiata* for dispersal abilities equivalent to the case of constant dispersal and the couple sets of demographic parameters characterizing the three biological situations considered: in all the
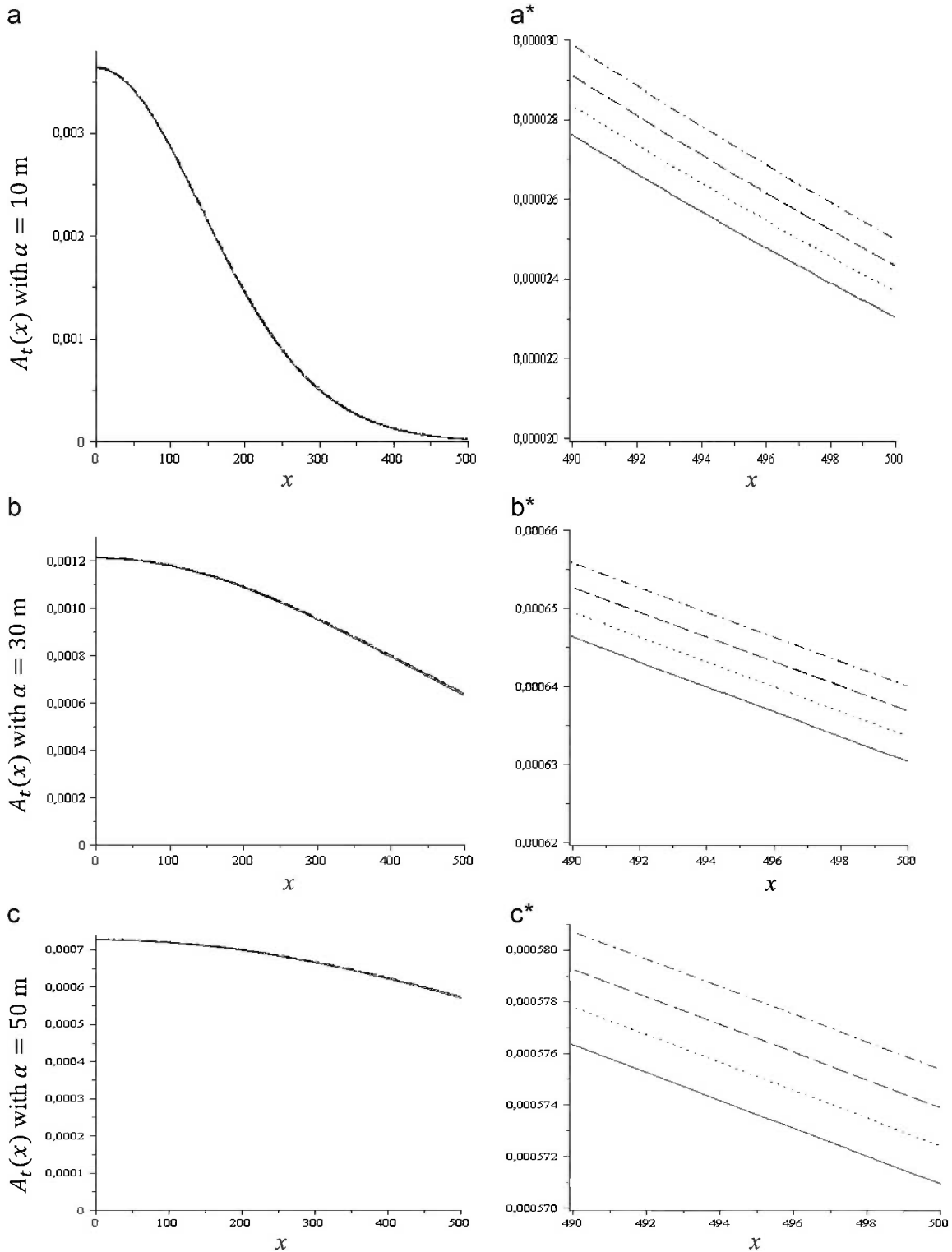
Fig. 4. Plots of adult densities $A_t(x)$ in the constant case $CD_{f_{a\_field}}$ (see Table 1) for $t=155$ (solid curves), $t=156$ (dot), $t=157$ (dash) and $t=158$ (dashdot) with three different values of the mean dispersal: (a) $\alpha=10$ m, (b) $\alpha=30$ m, and (c) $\alpha=50$ m. The curves in (a*), (b*) and (c*) show the edges of the curves in (a), (b) and (c), respectively.

cases, the invasion speed is higher with periodic dispersal than with constant dispersal except for conditions $(D_{50\%lab}, ND_{50\%lab})$ and $(D_{all\_bad}, ND_{all\_bad})$ where the population goes to extinction (Table 2). The largest increase was obtained in the case (D_{lab}, ND_{lab}) (situation 1 in Table 2): in this case c_{per} increased 146.9% of c_{cst}.

When *T. dimidiata* leaves a high-density habitat (situation 2 of Table 2), the field values of demographic parameters play a very important role; the maximum speed of invasion is expected in this case ($c_{per}=59.64$ m/w) when the probability of adult survival S_a of the non-dispersal period is based on field values (the parameter sets $(D_{lab}, ND_{S_a\_field})$); however, it is minimal when the fertility f_a of this non-dispersal period is that of the field (sets of parameters (D_{lab}, ND_{fa_field})). This corroborates the result of the maximum elasticity of c_{per} versus S_a obtained in Fig. 5.
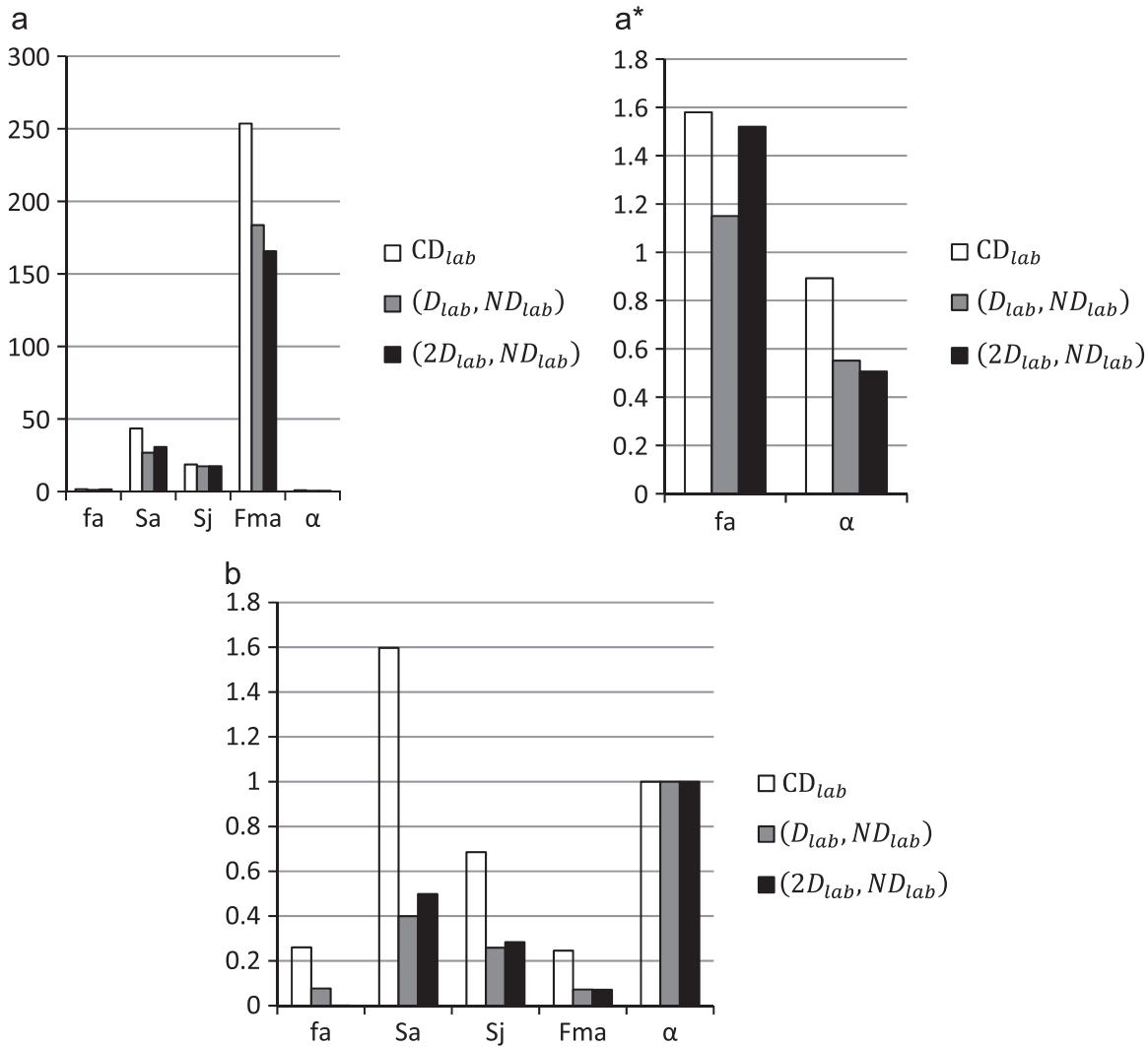
Fig. 5. Sensitivity and elasticity of the invasion speed to changes in each of the demographic and dispersal parameters for the constant case CD_{lab} (white bar), the periodic case (D_{lab}, ND_{lab}) with one season of dispersal (gray bar), and the periodic case $(2D_{lab}, ND_{lab})$ with two seasons of dispersal (black bar). See Table 1 for demographic and dispersal parameters. (a) sensitivity to f_a (fertility), S_a (adult survival probability), S_j (juvenile survival probability), F_{ma} (transition probability from juvenile to adult) and α (mean dispersal distance), (a*) sensitivity to f_a and α not apparent in (a); (b) elasticity.

The ecological situation where spatial dispersal is induced actively by host depletion or passively by hurricanes (both conditions correlated with low demography in situation 3), is characterized by invasion speeds in all cases higher than those obtained in situation 2 (dispersal correlated to high demography by intermediate of density-dependent dispersal). This reflects the fact that *T. dimidiata* may have a better invasive capacity when the period of non-dispersal is very favorable from demographic point of view (ND_{lab}). This improvement leads to an increase of c_{per} up to 139.6% of c_{cst}.

4.2.1. The effect of the duration of dispersal period

Extending the period of dispersal (dispersal in season A–S) while keeping the same capacity of dispersal in the case of one season A–J ($\alpha = 120$ m for a season and $\alpha = 60$ m in each season for the situation with two seasons) results in a decrease of the invasion speed of *T. dimidiata* (relative to a dispersal during only one season) of 55.8% in the situation 2 and 58.21% in situation 3. Despite the decrease in the rate of invasion with the longer period of dispersal, all demographic situations give invasion speeds above

the speed of invasion of the constant dispersal, except in the case where $c_{per} = 19.57$ m/w ($< c_{cst} = 26.80$ m/w).

In this new case extending the period of dispersal, the duration of the dispersal period (A–J) and non-dispersal periods (J–M, J–S and O–D) are not equal, and the invasion speeds corresponding to (D_i, ND_{lab}) of situation 3 remain greater than the speeds obtained with their permuted (D_{lab}, ND_j) of situation 2. This confirms that the population of triatomines has an important capacity of invasion when its demography is favorable during the period of non-dispersal.

4.3. Sensitivity analysis

The sensitivities and elasticities of the invasion speed c_l ($l = cst$ or per) to demographic parameters f_a, S_a, S_j, F_{ma} (given in Table 1) and to the scale of dispersal α are shown in Fig. 5. The patterns for the constant dispersal and the periodic dispersal are qualitatively similar. The invasion speed is most sensitive to F_{ma}, S_a and S_j. So, a good strategy for vector control may be to reduce transition probability from juvenile to adult stage (F_{ma}), adult survival (S_a) and juvenile survival (S_j).
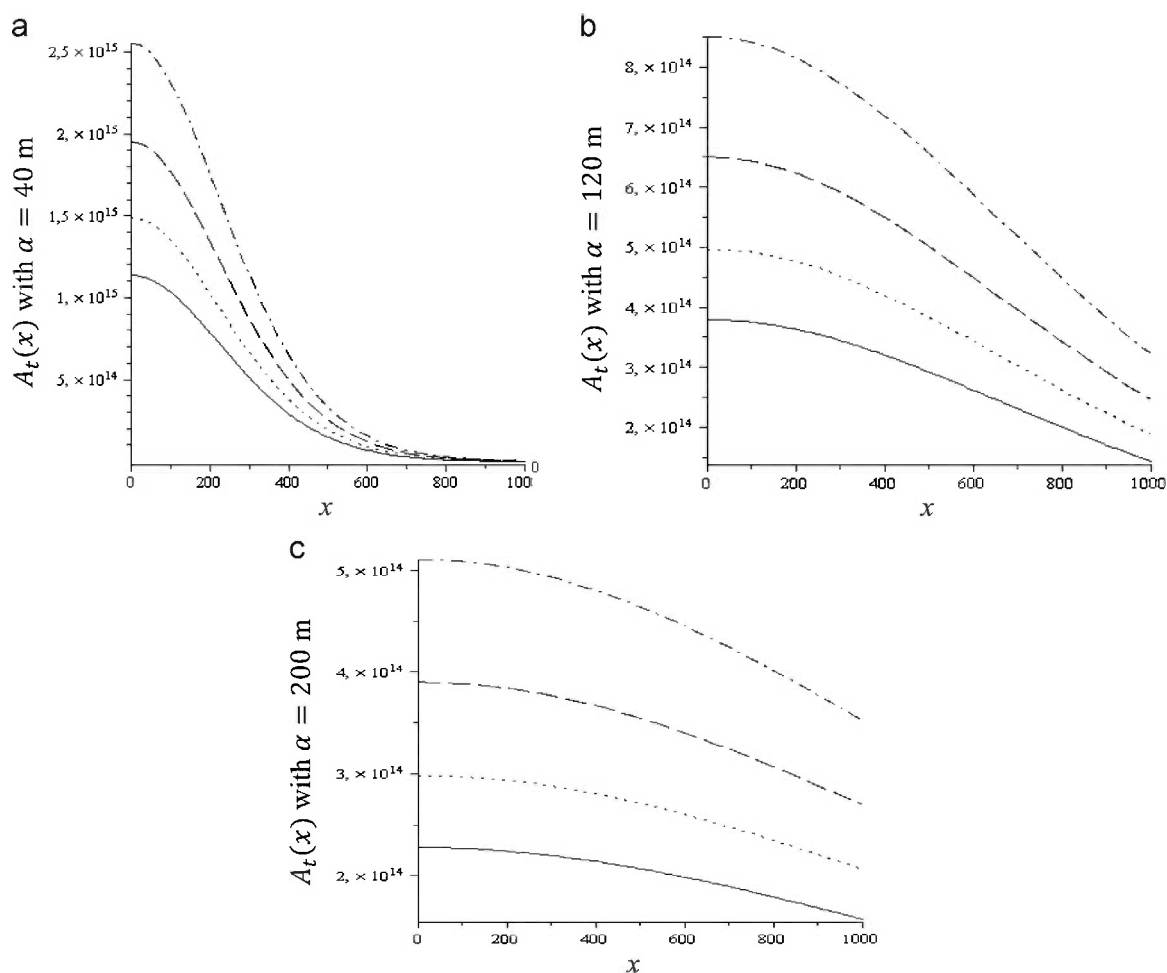
Fig. 6. Plots of adult densities $A_t(x)$ in the periodic case (see Table 1) for $t=155$ (solid curves), $t=156$ (dot), $t=157$ (dash) and $t=158$ (dashdot) with three different values of the mean dispersal distances α: (a) $\alpha = 40$, (b) $\alpha = 120$ and (c) $\alpha = 200$ m.
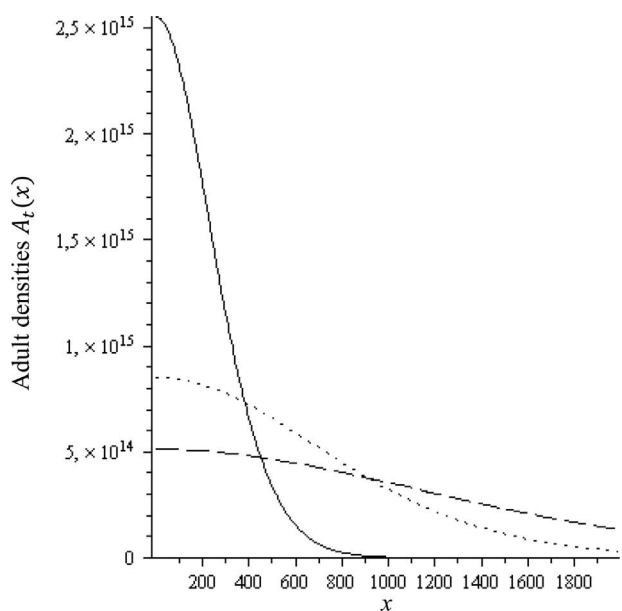
Fig. 7. Plots of adult densities $A_t(x)$ in the periodic case (see Table 1) for $t=158$, with $\alpha = 40$ (solid), $\alpha = 120$ (dot) and $\alpha = 200$ m (dash).

5. Discussion

The purpose of this study was to estimate the invasion speed of *T. dimidiata* in different ecological situations using an original mathematical method that allows accounting for two types of dispersal: a "constant dispersal", i.e. a weekly dispersal that does not vary within the year, and a "periodic dispersal", where weekly dispersal occurs only during a 3–6 month-periods in each year.

The constant and periodic models have been studied by considering various sets of demographic parameters representing different entomological and ecological situations. In all these situations, abundances were derived analytically by applying the properties of Chebyshev polynomials of the second kind and approximated asymptotically by applying the saddle point method. The expression of the invasion speed deduced from these approximations coincides with the formula obtained by Neubert and Caswell (2000). Accordingly, this methodology provides a new application of orthogonal polynomials which consists in a formal representation of the solutions of linear 2SIDE, an asymptotic behavior of the solutions, and the calculation of the invasion speed. This also, provides a biologically meaningful interpretation of the recurrence coefficients in the TTRR as those are formulated with respect basic demographic parameters.

The first major finding of this study is that for any given mean capacity of dispersal, the invasion speed is greater when dispersal is seasonal than when it occurs all year long. Furthermore, invasion speed increases with the shortening of the duration of the dispersal season. This has important implications for vector control because there exists an important variability of dispersal pattern between different triatomines species (see (Waleckx et al., 2015a) for a review), with some species such as *T. dimidiata*, showing clear seasonal pattern with a 3-months peak of

Table 2
The invasion speed in the constant and periodic cases for a dispersal period of one season and two seasons, calculated for different scenarios. The relative difference between, on one hand, the constant dispersal case and the periodic dispersal case, and on the other hand, between the one season periodic dispersal case and two seasons periodic dispersal case; they were calculated for different speeds for the sake of comparison.

Cases of spatial dispersal and different ecological situations		Set of demographic parameters	Invasion speed (m/w) for each demographic set (D_i, ND_j)	Relative difference between (D_i, ND_j) and CD_{Lab}	Invasion speed (m/w) for each demographic set $(2D_i, ND_j)$	Relative difference between $(2D_i, ND_j)$ and (D_i, ND_j)
Constant dispersal		CD_{lab}	26.80	–	--	–
		$CD_{50\%lab}$	extinction	–	–	–
		$CD_{f_{a\_field}}$	3.30	–	–	–
		CD_{all_bad}	extinction	–	–	–
Periodic dispersal	Situation 1	(D_{lab}, ND_{lab})	66.18	1.469	41.43	0.597
		$(D_{50\%lab}, ND_{50\%lab})$	extinction	–	–	–
		$(D_{all\_bad}, ND_{all\_bad})$	extinction	–	–	–
	Situation 2	$(D_{lab}, ND_{50\%f_a})$	56.05	1.091	35.92	0.560
		$(D_{lab}, ND_{50\%S_a})$	34.89	0.302	19.57	0.783
		$(D_{lab}, ND_{50\%S_j})$	39.36	0.469	27.51	0.431
		$(D_{lab}, ND_{50\%F_{ma}})$	56.43	1.106	35.96	0.569
		$(D_{lab}, ND_{f_{a\_field}})$	32.68	0.219	23.50	0.391
		$(D_{lab}, ND_{S_{a\_field}})$	59.64	1.225	36.96	0.614
	Situation 3	$(D_{50\%f_a}, ND_{lab})$	63.90	1.384	39.81	0.605
		$(D_{50\%S_a}, ND_{lab})$	45.43	0.695	31.25	0.454
		$(D_{50\%S_j}, ND_{lab})$	62.83	1.344	38.76	0.621
		$(D_{50\%F_{ma}}, ND_{lab})$	64.22	1.396	40.06	0.603
		$(D_{f_{a\_field}}, ND_{lab})$	60.70	1.265	37.33	0.626
		$(D_{S_{a\_field}}, ND_{lab})$	62.62	1.337	39.53	0.584

abundance observed in human dwellings (Barbu et al., 2009; Dumonteil et al., 2013). Our results indicate that such triatomine species with a seasonal dispersal are more likely to expand their geographical range than species dispersing all year long. In addition, sensitivity analysis suggests that vector control of such species with higher invading potential should focus primarily (if possible) on the transition from juvenile to adult, adult survival and to a lesser extent on the survival of juveniles. The second important finding of our study is that invasion speed is substantially greater (up to 34.7%) under the assumption of a dispersal correlated to low demography rates (either because of the absence of host or occurrence of hurricane) than when it is associated to high demography rates. Finally, the analysis of the distribution of adult dispersal distance shows that the maximum distance traveled varies with the dispersal capacity parameter α: the higher α the larger is the maximum distance reached, and the pattern is similar whatever the ecological situation considered here. We now discuss these main theoretical predictions with respect to the empirical knowledge of triatomines' dispersal that we found in the literature.

We have focused on *T. dimidiata* because dispersal was identified as a key factor of Chagas disease transmission to human by this non-domiciliated vector species (Gourbière et al., 2008), which has generated long-term field and modeling studies providing one of the rare quantitative assessments of triatomines dispersal in the field (see (Nouvellet et al., 2015) for a review). The marked effects of seasonality in our results suggest that it would be important for both fundamental and applied purposes to investigate the temporal variation in other species and to estimate their invasion capacity while accounting for such temporal pattern. Indeed, the literature shows that several triatomine species mainly disperse during short warmer periods and so we can anticipate such species to be more likely to expand their geographical range than other species dispersing all year long. In North America the species *T. protacta* was found to show the maximum natural dispersal activity in July and August with movements confined to a thermo-period of 15.5 °C to 24.4 °C

(Wood, 1967). Zeledón (1975) claims that warmer temperatures in countries with marked seasons seem to stimulate the dispersal activity of certain species which explains, at least in part, the increase in the number of acute Chagas disease cases during spring and summer. Dumonteil et al. (2002) documented strong seasonal variations in *T. dimidiata* populations, with a higher abundance during the hot and dry season in April–June, but reduced year-round colonization of houses; this feature plus the analysis of the developmental stage structure found, suggest that flying adults seasonally invade houses thus playing an important role in transmission of *T. cruzi* to humans. The relationship between temperature and dispersal in triatomines seems to have a physiological basis. For *Dipetalogaster maximus,* when temperature rises from 30 to 37 °C, an energy supply for muscle activity during flight is enhanced (Scaraffia and Gerez De Burgos, 2000). (Naiff et al. 1998) found in urban Manaus (Brazil) that *P. geniculatus* males were significantly more frequent in the dry season. Schofield et al. (1992) believe that in *T. infestans* temperature influences not only the proportion of bugs flying but also the distance flown. (Vazquez Prokopec et al. 2006) developed an empirical model of flight initiation and predicted that the flight dispersal of *T. infestans* would peak in summer; when winds were < 5 km/h, the arrival of adult *T. infestans* at the light traps was significantly associated with maximum temperature and relative humidity. Mac Cord and d'Almeida (1986) observed that fed *T. infestans* exposed to 30 °C for four hours, disperse from the eighth day of starvation.

We also established that the invasion speed is substantially greater when the dispersal period is correlated to low demographic rates, which could arise as a result of an absence of hosts or starvation. This result is in concordance with the experimental works on the influence of starvation on dispersal. Mac Cord and d'Almeida (1986) found that the length of the starvation period had more influence on triatomine dispersal than temperature. These conclusions were later corroborated by Lehane et al. (1992), who determined that flight initiation in *T. infestans* is associated with low nutritional status and increases with rising temperature. Lehane et al. (1992) also developed a predictive model for the

probability of flight initiation and concluded that flight would be rare during colder months ($< 20°C$) but that 5–10% of the population of an infested house would fly on any given night during the hotter months when temperature approaches $30°C$; however, if bug nutritional status falls significantly, this proportion could be expected to rise to 30%. Similar conclusions were arrived at in the case of *T. protracta*: flights occurred when starved bugs became stimulated by periods of above the average summer temperatures (Sjogren and Ryckman, 1966). We note the importance of wind (which can lead to low demography in the presence of hurricanes), that was also found to be associated with the dispersal of *R. prolixus* (D'Ascoli and Gómez-Núñez, 1966) and of *T. dimidiata* (Dumonteil et al., 2004).

Our models show that invasion speed also depends on the dispersal capacity of triatomines, i.e. the dispersal kernel, which varies with respect to species. For *T. dimidiata,* our analysis of adult distance distribution shows that the higher the mean dispersal capacity, α, the larger the maximum distance reached. For other species, *P. megistus* was recognized by (Miles 1976) as able to disperse for long distances in direction to houses, and confirmed by (Forattini et al. 1977). *T. sherlocki* was never recorded to fly while *T. infestans* and *R. prolixus* (as well as other triatomine species) fly readily; these differences were related to good/poor structures associated with locomotors abilities as well as to a physiological basis (Gringorten and Friend, 1979). Despite *T. sherlocki* was never recorded to fly, *T. juazeirensis* (a very related species) is an excellent flier and laboratory-bred hybrids between these two species had intermediate dispersal capacity (Almeida et al., 2012).

The invasion speed of *T. cruzi* has been examined by Crawford et al., (2013) under different vector migration scenarios. For no preferred direction of migration, the invasion speed of the epidemic ranged from 4.05 km/yr to 8.45 km/yr (or from 78 m/w to 162.5 m/w). When vectors migrate with a preferred direction, this range becomes 2.56 km/yr to 10.74 km/yr (or 50 m/w to 206.5 m/w). We examined the invasion speed of *T. dimidiata* in periodic environments under different biological situations; in the most realistic periodic case (three months of dispersal) the invasion speed ranged from 33 m/w to 64 m/w. The dispersal kernel and field studies showed that 44% of the adults have a capacity to travel farther than 100 m in a single flight, but their invasion speed was low. This is due to seasonality and the low values of certain demographic parameters (e.g., maturation $F_{ma}=0.026$). In the study of Crawford et al., (2013) this is due, for instance, to the assumption that triatomines can disperse only for a maximum of 5 weeks and maturation rate which affects the dispersal rate. The invasion speeds carried out from the (CA) model can be viewed as upper bounds for the (2SIDE) model since the epidemic spreads via two triatomines (by dispersal, migration and infection rates) and two hosts (by infection rates). Accordingly, the estimates of the invasion speed in Crawford et al., (2013) and in our modeling approache seem to be reasonable.

Our sensitivity analysis suggests that vector control of such species with higher invading potential should focus primarily (if possible) on the transition from juvenile to adult, and on adult and juvenile survival. Very little data is available in literature addressing the question about differential effect of insecticides on the triatomine's developmental stage. Indeed, most papers just use one nymphal instar (present World Health Organization recommendation is to use only 1st instars) and when they use more instars usually the type and number of each are not given, and/or the results do not discriminate among nymphal stages. When dieldrin was used (although it is not used any more) all the adults died but only 33% of the fifth instar nymphs died after a 48 h exposure to filter papers with a concentration of 1.6% dieldrin (Nocerino, 1975). Therefore, our study suggests that the effect of insecticides on survival of different insect stages should be investigated.

Our analysis shows that a more efficient control may consist in disturbing the transition from juvenile to adult stage. One possibility may be to use juvenile-hormone mimics. The juvenile-hormone mimics, such as Precocenes, are safe to use but slow-acting and active only on a few stages (Schofield, 1985). Garcia et al. (1987) indicate that Precocene and Azadirachtin are effective inhibitors of molting and reproduction in *R. prolixus*; however, they mention that the time of application is critical and only applications of these compounds early in the inter-molting period cause their effects in nymphs. In general Proallatotoxins, and particularly Precocenes, reveal significant effects on feeding, molting cycle (inducing precocious metamorphosis and ecdysial stasis), and reproduction in *R. prolixus*, apparently based on the *corpus allatum* cytotoxic effect and on the ecdysteroid biosynthesis in prothoracic glands and ovaries (Azambuja and Garcia, 1987). Finally, juvenile-hormone mimics tend to be highly specific resulting in an unattractively small market for commercial products (Patterson and Schwarz, 1977) as cited in (Schofield, 1985).

To conclude, our work shows that seasonal variation in the dispersal process cannot be neglected when estimating the invasion capacity of triatomines and, presumably, others species. While the models used in this paper consider a deterministic environment (i.e. constant or with seasonal variations), demographic parameters are usually influenced by environmental stochasticity (unpredictable variation) in the field, which was actually recently proposed for triatomines (Menu et al., 2010; Pelosse et al., 2013). How such unpredictable environmental variations affect insect demography and/or the dispersal and their invasion speed remains an open question. Such further developments would represent a natural extension of the framework presented in the present study, and of the use of orthogonal polynomials and their asymptotic properties, whereby demographic and dispersal parameters vary with time.

Acknowledgments

Appendix A

This appendix contains the proofs and calculus leading to approximations of adult density $A_t(x)$ and the invasion speed c_{cst} in the case of a constant environment. It consists of six sections: the first section deals with the properties of the exponential transform; the second and third sections are about orthogonal polynomials and their application in the general case and, finally, the fourth, fifth and sixth sections are reserved to the calculus of the approximations of $A_t(x)$ and c_{cst} in the particular case of a constant environment.

5.1. A.1. The exponential transform

The exponential transform for a function f is defined by (see (Kot and Neubert, 2008) and the references therein)

$$\hat{f}(s) = \int_{-\infty}^{+\infty} f(x)e^{sx}dx \tag{A.1}$$

and its inverse is

$$f(x) = \frac{1}{2\pi i}\int_{\rho-i\infty}^{\rho+i\infty} \hat{f}(s)e^{-sx}ds. \tag{A.2a}$$

The constant ρ is chosen so that the integration is along a vertical line within the vertical strip of convergence of the transform.

The convolution product is defined as

$$(f * g)(x) = \int_{-\infty}^{+\infty} f(y-x)g(y)dy \tag{A.2b}$$

and satisfies the property

$$\widehat{f * g}(s) = \hat{f}(s)\hat{g}(s). \tag{A.2c}$$

For a natural number n, we put $f^{*(n+1)} = f * f^{*(n)}$ and by convention $f^{*(0)} = \delta$ (the Dirac distribution).

Remark A.1. Let s be a real number. Then $\hat{f}(is)$ is the Fourier transform of $f(x)$ defined as

$$\hat{f}(is) = \int_{-\infty}^{+\infty} f(x)e^{isx}dx \tag{A.3}$$

and the inverse transform is

$$f(x) = \frac{1}{2\pi}\int_{-\infty}^{+\infty} \hat{f}(is)e^{-isx}ds = \frac{1}{2\pi i}\int_{-i\infty}^{i\infty} \hat{f}(s)e^{-sx}ds \tag{A.4}$$

If $f(x)$ is positive, then the existence of $\hat{f}(0)$ implies the existence of $\hat{f}(is)$ for every s real according to the inequality

$$\left|\hat{f}(is)\right| \le \hat{f}(0) \ \text{for} \ s \in \mathbb{R}. \tag{A.5}$$

We need the following notions (see (Murray, 1984), Chap.1):

Definition A.1. We say that $f_t(z)$ is equivalent to $g_t(z)$ when $t \to +\infty$ and we note $f_t(z) \sim g_t(z)$ if

$$\lim_{t\to+\infty}\frac{f_t(z)}{g_t(z)} = 1 \tag{A.6a}$$

or

$$\forall \varepsilon > 0, \exists t_0 \in \mathbb{N} \, t \ge t_0 \Rightarrow |f_t(z) - g_t(z)| < \varepsilon|g_t(z)| \tag{A.6b}$$

The equivalence is uniform if t_0 is independent of z.

Proposition A.1. ((Murray, 1984), p.34 formula 2.33).

Suppose that the functions $g(s), h(s), h'(s)$ and $h''(s)$ are real and continuous for all real s. Assume that $h(s) \le h(0)$ for all real s, $h'(0) = 0$, $h''(0) < 0$, $g(0) \ne 0$ and $g(s) = g(0) + sg'(0) + O(s^2)$. Then we have the asymptotic approximation as $t \to \infty$

$$\int_{-\infty}^{+\infty} e^{th(s)}g(s)ds \sim \frac{g(0)e^{th(0)}\sqrt{2\pi}}{\sqrt{|h''(0)|t}} \tag{A.7}$$

Note that, if $g(s) > 0$ in a neighborhood of $s = 0$, then

$$\int_{-\infty}^{+\infty} e^{th(s)}|g(s)|ds \sim \int_{-\infty}^{+\infty} e^{th(s)}g(s)ds \tag{A.8}$$

Proposition A.2. Let g and h as in proposition A.1. with $g(s) > 0$ in a neighborhood of $s = 0$. Suppose that $Q_t(s) \sim e^{th(s)}g(s)$ uniformly as $t \to \infty$, then

$$\int_{-\infty}^{+\infty} Q_t(s)\cos(sx)ds \sim \int_{-\infty}^{+\infty} e^{th(s)}g(s)\cos(sx)ds. \tag{A.9}$$

Proof. Let $\varepsilon > 0$ and $\varepsilon_1 > 0$. As $Q_t(s) \sim e^{th(s)}g(s)$ and by using definition A.1., it exists a $t_0(\varepsilon/(1+\varepsilon_1)) \ge 0$ such that, for $t \ge t_0(\varepsilon/(1+\varepsilon_1))$ we have

$$\left|\int_{-\infty}^{+\infty} Q_t(s)\cos(sx)ds - \int_{-\infty}^{+\infty} e^{th(s)}g(s)\cos(sx)ds\right|$$

$$= \left|\int_{-\infty}^{+\infty} \left(Q_t(s) - e^{th(s)}g(s)\right)\cos(sx)ds\right|$$

$$\le \int_{-\infty}^{+\infty} \left|Q_t(s) - e^{th(s)}g(s)\right|\left|\cos(sx)\right|ds$$

$$\le \int_{-\infty}^{+\infty} \left|Q_t(s) - e^{th(s)}g(s)\right|ds \le \frac{\varepsilon}{(1+\varepsilon_1)}\int_{-\infty}^{+\infty} \left|e^{th(s)}g(s)\right|ds.$$

As g is positive in a neighborhood of $s = 0$, we can write

$$\int_{-\infty}^{+\infty} e^{th(s)}g(s)\cos(sx)ds \sim \int_{-\infty}^{+\infty} e^{th(s)}g(s)ds \sim \int_{-\infty}^{+\infty} \left|e^{th(s)}g(s)\right|ds.$$

So for $t \ge t_1(\varepsilon_1, x)$ we have

$$(1-\varepsilon_1)\left|\int_{-\infty}^{+\infty} e^{th(s)}g(s)\cos(sx)ds\right| \le \int_{-\infty}^{+\infty} |e^{th(s)}g(s)|\,ds$$

$$\le (1+\varepsilon_1)\left|\int_{-\infty}^{+\infty} e^{th(s)}g(s)\cos(sx)ds\right|.$$

Thus, for $t \ge \max(t_1(\varepsilon_1, x), t_0(\varepsilon/(1+\varepsilon_1)))$ we obtain

$$\left|\int_{-\infty}^{+\infty} Q_t(s)\cos(sx)ds - \int_{-\infty}^{+\infty} e^{th(s)}g(s)\cos(sx)ds\right|$$

$$\le \varepsilon\left|\int_{-\infty}^{+\infty} e^{th(s)}g(s)\cos(sx)ds\right|,$$

which is the equivalence in proposition A.2.

5.2. A.2. Orthogonal polynomials

A polynomial set $\{P_t\}_{t \ge 0}$, with degree$(P_t) = t$ for $t \ge 0$, is an orthogonal polynomial set (OPS) with respect to a linear functional $\mathcal{L}$, if for every non negative integers t_1 and t_2 we have

$$\mathcal{L}(P_{t_1}P_{t_2}) = 0 \quad \text{if} \quad t_1 \ne t_2 \quad \text{and} \quad \mathcal{L}\left(P_{t_1}^2\right) \ne 0. \tag{A.10}$$

Or equivalently, they satisfy the so called three term recurrence relation (TTRR)

$$\begin{cases} XP_t(X) = a_{1,t}P_{t+1}(X) + a_{2,t}P_t(X) + a_{3,t}P_{t-1}(X), t \ge 0 \\ P_{-1}(X) = 0, P_0(X) = 1 \end{cases} \tag{A.11}$$

with $a_{1,t}a_{3,t+1} \ne 0$ for $t \ge 0$. For more details see for instance (Chihara, 1978).

The connection between orthogonal polynomials and the solutions of Eq. (2a) is made by using the TTRR and the following result.

Proposition A.3. Let $\{V_t\}_{t \ge 0}$ be a sequence defined by

$$\begin{cases} V_{t+1} = \xi\xi_t V_t + \eta\eta_t V_{t-1} \quad \text{for} \quad t \ge 1 \\ V_0 \text{ and } V_1 \text{ known} \end{cases} \tag{A.12}$$

with ξ, η real numbers and $\{\xi_t\}_{t \ge 0}$, $\{\eta_t\}_{t \ge 0}$ real sequences such

that $\xi \eta \xi_t \neq 0$ for $t \geq 0$. Then,

$$V_t = (-i)^t \eta^{\frac{t}{2}} \left[V_0 F_t \left(i \frac{\xi}{\sqrt{\eta}} \right) + i(V_1 - \xi \xi_0 V_0) \eta^{-\frac{1}{2}} G_{t-1} \left(i \frac{\xi}{\sqrt{\eta}} \right) \right] \quad (A.13)$$

where $i^2 = -1$, $\{F_t\}_{t \geq 0}$ and $\{G_t\}_{t \geq 0}$ are polynomials defined by

$$\begin{cases} \xi_t X F_t(X) = F_{t+1}(X) + \eta_t F_{t-1}(X) \\ F_{-1}(X) = 0, F_0(X) = 1 \end{cases} \quad (A.14a)$$

and

$$\begin{cases} \xi_{t+1} X G_t(X) = G_{t+1}(X) + \eta_{t+1} G_{t-1}(X) \\ G_{-1}(X) = 0, G_0(X) = 1 \end{cases} \quad (A.14b)$$

with degree(F_t)=degree(G_t).

Furthermore, if $\eta_t \neq 0$ for $t \geq 1$, then the polynomials $\{F_t\}_{t \geq 0}$ and $\{G_t\}_{t \geq 0}$ are orthogonal.

Proof. We proceed by induction on t. For $t = 0$ it is easily seen that the assertion Eq. (A.13) is satisfied. Assume that Eq. (A.13) is true until t and let us prove it for $(t+1)$.

The substitution of V_t and V_{t-1} in Eq. (A.12) yields:

$$V_{t+1} = \xi \xi_t (-i)^t \eta^{\frac{t}{2}} \left[V_0 F_t \left(i \frac{\xi}{\sqrt{\eta}} \right) + i(V_1 - \xi \xi_0 V_0) \eta^{-\frac{1}{2}} G_{t-1} \left(i \frac{\xi}{\sqrt{\eta}} \right) \right]$$
$$+ \eta \eta_t (-i)^{t-1} \eta^{\frac{(t-1)}{2}} \left[V_0 F_{t-1} \left(i \frac{\xi}{\sqrt{\eta}} \right) + i(V_1 - \xi \xi_0 V_0) \eta^{-\frac{1}{2}} G_{t-2} \left(i \frac{\xi}{\sqrt{\eta}} \right) \right]$$

$$= (-i)^{t+1} \eta^{\frac{(t+1)}{2}} \left[V_0 \left(\xi_t i \frac{\xi}{\sqrt{\eta}} F_t \left(i \frac{\xi}{\sqrt{\eta}} \right) - \eta_t F_{t-1} \left(i \frac{\xi}{\sqrt{\eta}} \right) \right) \right.$$
$$\left. + i(V_1 - \xi \xi_0 V_0) \eta^{-\frac{1}{2}} \left(\xi_t i \frac{\xi}{\sqrt{\eta}} G_{t-1} \left(i \frac{\xi}{\sqrt{\eta}} \right) - \eta_t G_{t-2} \left(i \frac{\xi}{\sqrt{\eta}} \right) \right) \right].$$

Now, by using Eqs. (A.14) we find

$$V_{t+1} = (-i)^{t+1} \eta^{\frac{(t+1)}{2}} \left[V_0 F_{t+1} \left(i \frac{\xi}{\sqrt{\eta}} \right) + i(V_1 - \xi \xi_0 V_0) \eta^{-\frac{1}{2}} G_t \left(i \frac{\xi}{\sqrt{\eta}} \right) \right],$$

which is the desired relation.

The sets $\{F_t\}_{t \geq 0}$ and $\{G_t\}_{t \geq 0}$ are polynomials such that degree(F_t) = degree(G_t) = t. This can be easily verified by induction from Eq. (A.14a) and Eq. (A.14b), respectively.

As $\xi_t \neq 0$ for $t \geq 0$ and $\eta_t \neq 0$ for $t \geq 1$ we conclude that $\frac{1}{\xi_t} \frac{\eta_{t+1}}{\xi_{t+1}} \neq 0$ for $t \geq 0$. So, from Eq. (A.11), the polynomials $\{F_t\}_{t \geq 0}$ and $\{G_t\}_{t \geq 0}$ are orthogonal.

Remark A.2. We have $F_t(-X) = (-1)^t F_t(X)$ and $G_t(-X) = (-1)^t G_t(X)$. This means that if t is even (resp. odd) the polynomials are even (resp. odd), they are called symmetric. See ((Chihara, 1978), Th.4.3, p.21). This implies that $F_t(X)$ and $G_t(X)$ can be expended as:

$$F_t(X) = \sum_{l=0}^{[t/2]} f_{t,l} X^{t-2l} \quad (A.15)$$

and

$$G_t(X) = \sum_{l=0}^{[t/2]} g_{t,l} X^{t-2l} \quad (A.16)$$

where $f_{t,l}$ and $g_{t,l}$ are real coefficients. These expansions are used later to write population densities (see Eqs. (A.29a) and (B.6)).

Remark A.3. The polynomials $\{G_t\}$ are called the associated polynomials and they are obtained from the polynomials $\{F_t\}$ by a shift on the coefficients (ξ_t, η_t). ((Van Assche, 1987), p.8).

5.3. A.3. Application in general case

The exponential transform applied to Eq. (2a) in text, assuming that $\hat{A}_0(s)$, $\hat{J}_0(s)$ and $\left\{ \hat{k}_{lm,t}(s) \right\}_{t \geq 0}$ exist for $s \in I \subset \mathbb{C}$, yields to the following system

$$\begin{cases} \hat{J}_{t+1}(s) = b_{11,t} \hat{k}_{11,t}(s) \hat{J}_t(s) + b_{12,t} \hat{k}_{12,t}(s) \hat{A}_t(s) \\ \hat{A}_{t+1}(s) = b_{21,t} \hat{k}_{21,t}(s) \hat{J}_t(s) + b_{22,t} \hat{k}_{22,t}(s) \hat{A}_t(s). \\ \qquad \hat{J}_0(s) \text{ and } \hat{A}_0(s) \text{ known} \end{cases} \quad (A.17)$$

Remark that $\hat{k}_{lm,t}(0) = 1$ (because they are probability densities), and that, it is reasonable to assume $\hat{J}_0(0)$ and $\hat{A}_0(0)$ finite (because they are the total of juveniles and the total of adults, at time $t=0$ in the whole habitat, respectively). So, $0 \in I$, and this implies that we can take the imaginary axis as a path of integration in the inverse exponential transform (remark A.1).

Notice that for $s = 0$, the quantity $\hat{A}_t(0)$ is the population size of adults at time t in the whole habitat. We denote by λ_t the per capita growth rate at time t for the adults in the whole habitat. We have:

$$\lambda_t = \hat{A}_{t+1}(0)/\hat{A}_t(0). \quad (A.18a)$$

Its geometric mean is

$$(\lambda_0 \lambda_1 \lambda_2 \ldots \lambda_{t-1})^{1/t} = \left(\hat{A}_t(0)/\hat{A}_0(0) \right)^{1/t} \quad (A.18b)$$

with limit

$$\lambda = \lim_{t \to \infty} (\lambda_0 \lambda_1 \lambda_2 \ldots \lambda_{t-1})^{1/t}. \quad (A.18c)$$

Now, we establish the TTRR (of the form Eq. (A.12)) satisfied by $\hat{A}_t$ and $\hat{J}_t$.

To simplify calculus we put

$$a_t(s) = b_{11,t} \hat{k}_{11,t}(s) \quad (A.19a)$$

$$b_t(s) = b_{12,t} \hat{k}_{12,t}(s) \quad (A.19b)$$

$$c_t(s) = b_{21,t} \hat{k}_{21,t}(s) \quad (A.19c)$$

$$d_t(s) = b_{22,t} \hat{k}_{22,t}(s). \quad (A.19d)$$

System Eq. (A.17), where the variable s is omitted, takes the form:

$$\begin{cases} \hat{J}_{t+1} = a_t \hat{J}_t + b_t \hat{A}_t \\ \hat{A}_{t+1} = c_t \hat{J}_t + d_t \hat{A}_t. \\ \hat{A}_0 \text{ and } \hat{J}_0 \text{ known} \end{cases} \quad (A.20)$$

Put $(t-1)$ instead of t in the equations to get

$$\begin{cases} \hat{J}_t = a_{t-1} \hat{J}_{t-1} + b_{t-1} \hat{A}_{t-1} \\ \hat{A}_t = c_{t-1} \hat{J}_{t-1} + d_{t-1} \hat{A}_{t-1} \end{cases} \quad (A.21)$$

The elimination of $\hat{J}_{t-1}$ in the first equation and of $\hat{A}_{t-1}$ in the second one leads to the system

$$\begin{cases} c_{t-1} \hat{J}_t = a_{t-1} \hat{A}_t + (c_{t-1} b_{t-1} - a_{t-1} d_{t-1}) \hat{A}_{t-1} \\ b_{t-1} \hat{A}_t = d_{t-1} \hat{J}_t + (c_{t-1} b_{t-1} - a_{t-1} d_{t-1}) \hat{J}_{t-1} \end{cases} \quad (A.22)$$

Finally, eliminating $\hat{A}_t$ and $\hat{A}_{t-1}$ (resp. $\hat{J}_t$ and $\hat{J}_{t-1}$) from the first (resp. second) equation of Eq. (A.22) by using the second (resp. first) equation of Eq. (A.22), we obtain, for $t \geq 1$, the two TTRR

$$\begin{cases} b_{t-1} \hat{J}_{t+1} = (b_{t-1} a_t + b_t d_{t-1}) \hat{J}_t + b_t (c_{t-1} b_{t-1} - a_{t-1} d_{t-1}) \hat{J}_{t-1} \\ \qquad \hat{J}_0 \text{ and } \hat{J}_1 = a_0 \hat{J}_0 + b_0 \hat{A}_0 \text{ known} \end{cases} \quad (A.23a)$$

and

$$\begin{cases} c_{t-1} \hat{A}_{t+1} = (a_{t-1} c_t + d_t c_{t-1}) \hat{A}_t + c_t (c_{t-1} b_{t-1} - a_{t-1} d_{t-1}) \hat{A}_{t-1} \\ \qquad \hat{A}_0 \text{ and } \hat{A}_1 = c_0 \hat{J}_0 + d_0 \hat{A}_0 \text{ known} \end{cases} \quad (A.23b)$$

The relations Eq. (A.23a) and Eq. (A.23b) are of the form Eq. (A.12). For instance, for Eq. (A.23b) we have:

$$\xi\xi_t = \frac{a_{t-1}}{c_{t-1}}c_t + d_t \tag{A.24a}$$

$$\eta\eta_t = c_t\left(b_{t-1} - \frac{a_{t-1}}{c_{t-1}}d_{t-1}\right) \tag{A.24b}$$

$$V_0 = \hat{A}_0 \tag{A.24c}$$

$$V_1 = c_0\hat{J}_0 + d_0\hat{A}_0. \tag{A.24d}$$

Proposition A.3 and Eq. (A.23b) allow to express $\hat{A}_t$ by orthogonal polynomials for a large class of systems of type Eq. (A.17). Therefore, $A_t(x)$ can be expressed by orthogonal polynomials and the inverse exponential transform defined in Eq. (A.4).

Now from the asymptotic behavior of the orthogonal polynomials we find the asymptotic behavior of $\hat{A}_t(s)$, and then applying the steepest descent method to the integral in Eq. (A.4), we deduce the asymptotic behavior for $A_t(x)$.

5.4. A.4. Constant model

Next we show how the system (2a), with $\mathbf{B}_t = \mathbf{B}$ and $\mathbf{K}_t = \mathbf{K}$, is intimately related to Chebyshev polynomials of the second kind denoted $\{U_t\}_{t\geq 0}$ and defined by the TTRR:

$$\begin{cases} 2XU_t(X) = U_{t+1}(X) + U_{t-1}(X) \\ U_{-1}(X) = 0, U_0(X) = 1 \end{cases}. \tag{A.25}$$

They also have the expressions, see ((Magnus et al., 1966), p.257),

$$U_t(X) = \sum_{l=0}^{[t/2]} (-1)^l \binom{t-l}{l}(2X)^{t-2l} \tag{A.26a}$$

and

$$U_t(X) = \frac{\left(X+\sqrt{X^2-1}\right)^{t+1} - \left(X-\sqrt{X^2-1}\right)^{t+1}}{2\sqrt{X^2-1}}. \tag{A.26b}$$

In the constant case, the TTRR of $\hat{A}_t(s)$ is deduced from Eq. (A.23b) as follows

$$\begin{cases} \hat{A}_{t+1}(s) = 2\xi(s)\hat{A}_t(s) + \eta(s)\hat{A}_{t-1}(s) & t \geq 1 \\ \hat{A}_0(s) \text{ and } \hat{A}_1(s) = b_{21}\hat{k}_{21}(s)\hat{J}_0(s) + b_{22}\hat{k}_{22}(s)\hat{A}_0(s) \text{ known} \end{cases} \tag{A.27}$$

where

$$2\xi(s) = b_{11}\hat{k}_{11}(s) + b_{22}\hat{k}_{22}(s) \tag{A.28a}$$

and

$$\eta(s) = b_{12}b_{21}\hat{k}_{12}(s)\hat{k}_{21}(s) - b_{11}b_{22}\hat{k}_{11}(s)\hat{k}_{22}(s). \tag{A.28b}$$

Proposition A.4. The adults' density is

$$A_t = \sum_{l=0}^{[\frac{t}{2}]} \left(\frac{t-l}{l}\right)\left[A_0 * (b_{11}k_{11} + b_{22}k_{22}) + \frac{t-2l}{t-l}(b_{21}k_{21}*J_0 - b_{11}k_{11}*A_0)\right]$$

$$*(b_{11}k_{11} + b_{22}k_{22})^{*(t-1-2l)}$$

$$* (b_{12}b_{21}k_{12}*k_{21} - b_{11}b_{22}k_{11}*k_{22})^{*(l)} \tag{A.29a}$$

where the variable x is omitted to simplify notation and $\binom{t}{l} = \frac{t!}{l!(t-l)!}$ denote binomial coefficients.

Proof. Applying proposition A.3 to Eq. (A.27) with $(\xi, \xi_t, \eta, \eta_t) = (\xi(s), 2, \eta(s), 1)$, yields to the equality

$$\hat{A}_t(s) = \eta^{\frac{t}{2}}(s)(-i)^t\left[\hat{A}_0(s)U_t\left(\frac{i\xi(s)}{\sqrt{\eta(s)}}\right) + i\left(b_{21}\hat{k}_{21}(s)\hat{J}_0(s)\right.\right.$$

$$\left.\left. - b_{11}\hat{k}_{11}(s)\hat{A}_0(s)\right)\eta^{-\frac{1}{2}}(s)U_{t-1}\left(\frac{i\xi(s)}{\sqrt{\eta(s)}}\right)\right] \tag{A.29b}$$

where $\{U_t\}$ are Chebyshev polynomials of the second kind.

From Eq. (A.26a) and knowing that $\left(\frac{t-1-l}{l}\right) = \frac{t-2l}{t-l}\left(\frac{t-l}{l}\right)$, the relation Eq. (A.29b) (where we have omitted the variables to simplify notation) becomes

$$\hat{A}_t = \sum_{l=0}^{[\frac{t}{2}]} \left(\frac{t-l}{l}\right)\left[2\xi\hat{A}_0 + \frac{t-2l}{t-l}\left(b_{21}\hat{k}_{21}\hat{J}_0 - b_{11}\hat{k}_{11}\hat{A}_0\right)\right](2\xi)^{t-1-2l}\eta^l. \tag{A.29c}$$

Now by applying the inverse exponential transform and its convolution property, we obtain Eq. (A.29a). ∎

Remark A.5. Using Eq. (A.26b), $\hat{A}_t(s)$ in Eq. (A.29b) can be written as

$$\hat{A}_t(s) = C(s)\left(\xi(s) + \sqrt{\xi^2(s) + \eta(s)}\right)^t$$

$$+ \left(\hat{A}_0(s) - C(s)\right)\left(\xi(s) - \sqrt{\xi^2(s) + \eta(s)}\right)^t \tag{A.30}$$

with

$$C(s) = \frac{\hat{A}_1(s) - \hat{A}_0(s)\left(\xi(s) - \sqrt{\xi^2(s) + \eta(s)}\right)}{2\sqrt{\xi^2(s) + \eta(s)}} \tag{A.31}$$

5.5. A.5. Approximating adult density

Chebyshev polynomials have the following approximation

$$U_t(z) \sim \frac{1}{2}\frac{\left(z+\sqrt{z^2-1}\right)^{t+1}}{\sqrt{z^2-1}} \text{ for } z\notin[-1,1] \tag{A.32}$$

which can be deduced from Eq. (A.26b), or is a special case of Jacobi's polynomials approximation (Szegö, 1975).

We obtain then from Eq. (A.30) that

$$\hat{A}_t(s) \sim C(s)\left(\hat{M}_1(s)\right)^t \tag{A.33a}$$

where

$$\hat{M}_1(s) = \xi(s) + \sqrt{\xi^2(s) + \eta(s)}. \tag{A.33b}$$

By Eq. (A.4) and noting that the function $\hat{A}_t(is)$ is even we have

$$A_t(x) = \frac{1}{2\pi i}\int_{-i\infty}^{i\infty}\hat{A}(s)e^{-sx}ds = \frac{1}{2\pi}\int_{-\infty}^{+\infty}\hat{A}_t(is)e^{-isx}ds$$

$$= \frac{1}{2\pi}\int_{-\infty}^{+\infty}\hat{A}_t(is)\cos(sx)ds. \tag{A.34a}$$

From Eq. (A.33a) we get $\hat{A}_t(is) \sim C(is)\left(\hat{M}_1(is)\right)^t$. So, we can use proposition A.2 with $Q_t(s) = \hat{A}_t(is)$, $g(s) = C(is)$ and $h(s) = \ln\left(\hat{M}_1(is)\right)$ to obtain

$$A_t(x) \sim \frac{1}{2\pi}\int_{-\infty}^{+\infty}C(is)\left(\hat{M}_1(is)\right)^t\cos(sx)ds. \tag{A.34b}$$

The functions $C(is)$ and $\hat{M}_1(is)$ are even and by Eq. (A.4) we can write

$$A_t(x) \sim \frac{1}{2\pi}\int_{-\infty}^{+\infty}C(is)\left(\hat{M}_1(is)\right)^t\cos(sx)ds$$

$$\sim \frac{1}{2\pi i} \int_{-i\infty}^{i\infty} C(s)\left(\hat{M}_1(s)\right)^t e^{-sx} ds \tag{A.34c}$$

The steepest descent method is applied, as in (Kot and Neubert, 2008), to the integral $\frac{1}{2\pi i}\int_{-i\infty}^{i\infty} C(s)\left(\hat{M}_1(s)\right)^t e^{-sx} ds$, in order to arrive at the approximation

$$A_t(x) \sim \frac{C(s_0)e^{-xs_0}\left(\hat{M}_1(s_0)\right)^t}{\sqrt{2\pi|\kappa_1''(s_0)|t}} \tag{A.35}$$

where

$$\kappa_1(s) = \ln \hat{M}_1(s) \tag{A.36a}$$

and s_0 satisfies the equation

$$\frac{\hat{M}_1'(s_0)}{\hat{M}_1(s_0)} = \frac{x}{t}. \tag{A.36b}$$

5.6. A.6. Invasion speed

The invasion speed of the adults is defined as follows: choose a critical population level A_{cr} that defines the location of the front of the invasion. Then the location x_t of the invasion at time t is the furthest value of x where $A_t(x) = A_{cr}$. Between time zero and time t the location of the wave front has advanced a distance of $x_t - x_0$, and hence the average invasion speed by time t is given by $\frac{(x_t - x_0)}{t}$. The "invasion speed" is obtained by taking the limit: $\lim_{t\to\infty} \frac{(x_t - x_0)}{t} = \lim_{t\to\infty} \frac{x_t}{t}$.

Now, as the invasion speed is an asymptotic result, Eq. (A.35) is used for its calculation. By choosing a critical population size A_{cr}, if we set $A_t(x)$ to A_{cr} and solve Eq. (A.35) for the ratio x/t, we find that

$$\frac{x}{t} \sim \frac{1}{s_0}\left\{\ln\left[\hat{M}_1(s_0)\right] + \frac{1}{t}\ln\left[\frac{C(s_0)}{A_{cr}\sqrt{2\pi|\kappa_1''(s_0)|t}}\right]\right\}. \tag{A.37}$$

In the limit of large t, if the ratio x/t converges to a constant, then s_0 and $\kappa_1''(s_0)$ (as functions of s_0) converge to constants. Thus, by Eq. (A.37) the speed is

$$c_{cst} \equiv \lim_{t\to\infty} \frac{x}{t} = \frac{1}{s_0}\ln\left[\hat{M}_1(s_0)\right] \tag{A.38}$$

We have also, for large t from Eq. (A.36b) the equation

$$c_{cst} = \frac{\hat{M}_1'(s_0)}{\hat{M}_1(s_0)} \tag{A.39}$$

We can see easily that Eqs. (A.38) and (A.39) are equivalent to

$$\frac{d}{ds}\left[\frac{1}{s}\ln\left(\hat{M}_1(s)\right)\right]_{s=s_0} = 0 \quad \text{and} \quad c_{cst} = \frac{1}{s_0}\ln\left(\hat{M}_1(s_0)\right) \tag{A.40}$$

So, this means that

$$c_{cst} = \min_{\substack{s \in I \\ s > 0}} \frac{1}{s}\ln\left(\hat{M}_1(s)\right) \tag{A.41}$$

Appendix B

This appendix contains the proofs and calculus leading to approximations of adult density $A_t(x)$ and the invasion speed c_{per} in the case of a periodic environment. Calculus of the adult's density, in the case of a periodic environment is based primarily on calculus developed in Appendix A for the constant model.

Suppose the environment cycles, with a period T, through a set of T distinct phases (e.g., seasons). For each phase j, $j = 1, \ldots, T$, the demographic, dispersal and wave projection matrices are $\mathbf{B}_j$, $\mathbf{K}_j$ and $\mathbf{H}_j$ respectively. Over a complete environmental cycle, from t to $t+T$, the wave projection matrix is the product of the $\mathbf{H}_j$ (Caswell et al., 2011),

$$\mathbf{H}(s) = \mathbf{H}_T(s)\mathbf{H}_{T-1}(s)\ldots\mathbf{H}_1(s). \tag{B.1}$$

In fact we have

$$\hat{\boldsymbol{n}}_{t+T}(s) = \mathbf{H}(s)\hat{\boldsymbol{n}}_t(s) \tag{B.2}$$

Let r being the time of the census at the beginning of each phase ($r = 0\ldots T-1$), putting $tT+r$ instead of t in Eq. (B.2) gives, for a time step of T and initial condition $\hat{\boldsymbol{n}}_r(s)$, the underlying system

$$\hat{\boldsymbol{n}}_{(t+1)T+r}(s) = \mathbf{H}(s)\hat{\boldsymbol{n}}_{tT+r}(s) \tag{B.3}$$

which is a constant model similar to the system in Eq. (A.17). So, the previous results of "constant model" can be applied with initial condition $\boldsymbol{n}_r(x)$ and

$$\mathbf{H}(s) = \mathbf{H}(0) \circ \hat{\mathbf{K}}(s). \tag{B.4}$$

where $\mathbf{H}(0)$ is the demographic projection matrix and $\hat{\mathbf{K}}(s) = \int \mathbf{K}(x)exp(sx)dx$, $\mathbf{K}(x)$ is the dispersal matrix.

Put $\mathbf{H}(s) = \left(\hat{h}_{lm}(s)\right)$, then $\mathbf{H}(0) = \left(\hat{h}_{lm}(0)\right)$ and $\hat{\mathbf{K}}(s) = \left(\frac{\hat{h}_{lm}(s)}{\hat{h}_{lm}(0)}\right)$. A relation similar to relation Eq. (A.29b) (in the proof of proposition A.4) takes the form

$$\hat{A}_{tT+r} = \sum_{l=0}^{\left[\frac{t}{2}\right]}\binom{t-l}{l}\left[2\xi_1\hat{A}_r + \frac{t-2l}{t-l}\left(\hat{h}_{21}\hat{J}_r - \hat{h}_{11}\hat{A}_r\right)\right](2\xi_1)^{t-1-2l}\eta_1^l \tag{B.5}$$

with $2\xi_1 = \hat{h}_{11} + \hat{h}_{22}$ and $\eta_1 = \hat{h}_{12}\hat{h}_{21} - \hat{h}_{11}\hat{h}_{22}$.

By applying the inverse exponential transform in Eq. (B.5) we get an exact expression of $A_{tT+r}(x)$:

$$A_{tT+r} = \sum_{l=0}^{\left[\frac{t}{2}\right]}\binom{t-l}{l}\left[A_r*(h_{11}+h_{22}) + \frac{t-2l}{t-l}(h_{21}*J_r - h_{11}*A_r)\right]*$$
$$*(h_{11}+h_{22})^{*(t-1-2l)}*(h_{12}*h_{21}-h_{11}*h_{22})^{*(l)}. \tag{B.6}$$

As in the "constant model" above, we can write an approximation of $A_{tT+r}(x)$ and give the invasion speed. See Eq. (10) and Eq. (12) in text.

References

Abad-Franch, F., Diotaiuti, L., Gurgel-Gonçalves, R., Gürtler, R.E., 2013. Certifying the interruption of Chagas disease transmission by native vectors: cui bono? Mem. Inst. Oswaldo Cruz 108, 251–254.

Almeida, C.E., Oliveira, H.L., Correia, N., Dornak, L.L., Gumiel, M., Neiva, V.L., Harry, M., Mendonça, V.J., Costa, J., Galvão, C., 2012. Dispersion capacity of *Triatoma sherlocki*, *Triatoma juazeirensis* and laboratory-bred hybrids. Acta Trop. 122, 71–79.

Azambuja, Pd, Garcia, E.S., 1987. Short-and long-term effects of proallatotoxin (Ethoxyprecocene II) on *Rhodnius prolixus* females. Mem. Inst. Oswaldo Cruz 82, 247–251.

Barbu, C., Dumonteil, E., Gourbière, S., 2009. Optimization of control strategies for non-domiciliated Chagas disease vectors with seasonal infestation. PLoS Ntd. 3 (4), e416.

Barbu, C., Dumonteil, E., Gourbière, S., 2010. Characterization of the Dispersal of Non-Domiciliated *Triatoma dimidiata* through the Selection of Spatially Explicit Models. PLoS Negl. Trop. Dis. 4, e777.

Barbu, C., Dumonteil, E., Gourbière, S., 2011. Evaluation of spatially targeted strategies to control non-domiciliated *Triatoma dimidiata* vector of Chagas disease. PLoS Negl. Trop. Dis. 5, e1045.

Borges, É.C., Dujardin, J.-P., Schofield, C.J., Romanha, A.J., Diotaiuti, L., 2005. Dynamics between sylvatic, peridomestic and domestic populations of *Triatoma brasiliensis* (Hemiptera: Reduviidae) in Ceará State, Northeastern Brazil. Acta Trop. 93, 119–126.

Canals, M., Solís, R., Tapia, C., Ehrenfeld, M., Cattan, P., 1999. Comparison of some behavioral and physiological feeding parameters of *Triatoma infestans* Klug,

1834 and *Mepraia spinolai* Porter, 1934, vectors of Chagas disease in Chile. Mem. Inst. Oswaldo Cruz 94, 687–692.

Caswell, H., Neubert, M., Hunter, C., 2011. Demography and dispersal: invasion speeds and sensitivity analysis in periodic and stochastic environments. Theor. Ecol. 4, 407–421.

Catala, S., 1991. Biting rate of Triatoma infestans in Argentina. Med. Veter. Entomol. 5, 325–333.

Ceballos, L., Vazquez-Prokopec, G., Cecere, M., Marcet, P., Gürtler, R., 2005. Feeding rates, nutritional status and flight dispersal potential of peridomestic populations of Triatomainfestans in rural northwestern Argentina. Acta Trop. 95, 149–159.

Chihara, T.S., 1978. An Introduction to Orthogonal Polynomials. Gordon and Breach, New York.

Cissé, B., El Yacoubi, S., Gourbière, S., 2016. A cellular automaton model for the transmission of Chagas disease in heterogeneous landscape and host community. Appl. Math. Model. 40 (2), 782–794.

Collier, B., Bosque, C., Rodriguez, E., Rabinovich, J.E., 1977. The energy budget of *Triatoma phyllosoma* (Hemiptera, Reduviidae) under laboratory conditions. J. Med. Entomol. 14, 425–433.

Crawford, B.A., Kribs-Zaleta, C.M., 2013. Vector migration and dispersal rates for sylvatic Trypanosoma cruzi transmission. Ecol. Complex. 14, 145–156.

Crawford, B.A., Kribs-Zaleta, C.M., Ambartsoumian, G., 2013. Invasion speed in cellular automaton models for *T. cruzi* vector migration. Bull. Math. Biol. 75, 1051–1081.

D'Ascoli, A., Gómez-Núñez, J.C., 1966. Notas sobre los Medios de Dispersión del *Rhodnius prolixus*. Stal. Acta Cient. Venez. 17, 22–25.

Devillers, H., Lobry, J.R., Menu, F., 2008. An agent-based model for predicting the prevalence of *Trypanosoma cruzi* I and II in their host and vector populations. J. Theor. Biol. 255, 307–315.

Dumonteil, E., Ruiz-Piña, H., Rodriguez-Félix, E., Barrera-Pérez, M., Ramirez-Sierra, M.J., Rabinovich, J.E., Menu, F., 2004. Re-infestation of houses by *Triatoma dimidiata* after intra-domicile insecticide application in the Yucatan peninsula, Mexico. Mem. Inst. Oswaldo Cruz 99, 253–256.

Dumonteil, E., Nouvellet, P., Rosecrans, K., Ramirez-Sierra, M.J., Gamboa-Leon, R., Cruz-Chan, V., Rosado-Vallado, M., Gourbière, S., 2013. Eco-bio-social determinants for house infestation by non-domiciliated *Triatoma dimidiata* in the Yucatan peninsula, Mexico. PLoS Negl. Trop. Dis. 7, e2466.

Dumonteil, E., Gourbière, S., Barrera-Pérez, M., Rodriguez-Félix, E., Ruiz-Piña, H., Baños-Lopez, O., Ramirez-Sierra, M.J., Menu, F., Rabinovich, J.E., 2002. Geographic distribution of *Triatoma dimidiata* and transmission dynamics of *Trypanosoma cruzi* in the Yucatan peninsula of Mexico. Am. J. Trop. Med. Hyg. 67, 176–183.

Dunning Jr, J.B., Stewart, D.J., Danielson, B.J., Noon, B.R., Root, T.L., Lamberson, R.H., Stevens, E.E., 1995. Spatially explicit population models: current forms and future uses. Ecol. Appl. 5, 3–11.

Forattini, O.P., Ferreira, O.A., Silva, E.Od.R., Rabello, E.X., 1975. Aspectos ecológicos da tripanossomíase americana: VII-Permanência e mobilidade do Triatoma sordida em relação aos ecótopos artificiais. Rev. Saúde públ, 467–476.

Forattini, O.P., Ferreira, O.A., Silva, E.Od.Re, Rabello, E.X., 1977. Aspectos ecológicos da Tripanossomíase americana: VIII – Domiciliação de Panstrongylus megistus e sua presença extradomiciliar. Rev. Saúde Pública 11, 73–86.

Friend, W., Choy, C., Cartwright, E., 1965. The effect of nutrient intake on the development and the egg production of *Rhodnius prolixus* Ståhl (Hemiptera: Reduviidae). Can. J. Zool. 43, 891–904.

Galvão, C., Rocha, Dd.S., Jurberg, J., Carcavallo, R., 2001. Início da atividade de vôo em *Triatoma infestans* (Klug, 1834) e T. melanosoma Martínez, Olmedo & Carcavallo, 1987 (Hemiptera, Reduviidae). Mem. Inst. Oswaldo Cruz 96, 137–140.

Garcia, E.S., Feder, D., Gomes, J.E.P., Azambuja, Pd, 1987. Effects of precocene and azadirachtin in *Rhodnius prolixus*: some data on development and reproduction. Mem. Inst. Oswaldo Cruz 82, 67–73.

Gourbière, S., Dorn, P., Tripet, F., Dumonteil, E., 2012. Genetics and evolution of triatomines: from phylogeny to vector control. Heredity 108, 190–202.

Gourbière, S., Dumonteil, E., Rabinovich, J.E., Minkoue, M., Menu, F., 2008. Demographic and dispersal constraints for domestic infestation by non-domiciled Chagas disease vectors in the Yucatan Peninsula, Mexico. Am. J. Trop. Med. Hyg. 78, 133–139.

Gringorten, J., Friend, W., 1979. Haemolymph-volume changes in *Rhodnius prolixus* during flight. J. Exp. Biol. 83, 325–333.

Guhl, F., Pinto, N., Aguilera, G., 2009. Sylvatic triatominae: a new challenge in vector control transmission. Mem. Inst. Oswaldo Cruz 104, 71–75.

Gurevitz, J.M., Gaspe, M.S., Enríquez, G.F., Vassena, C.V., Alvarado-Otegui, J.A., Provecho, Y.M., Cueto, G.A.M., Picollo, M.I., Kitron, U., Gürtler, R.E., 2012. Unexpected failures to control Chagas disease vectors with pyrethroid spraying in northern Argentina. J. Med. Entomol. 49, 1379–1386.

Gürtler, R.E., Diotaiuti, L., Kitron, U., 2008. Commentary: Chagas disease: 100 years since discovery and lessons for the future. Int. J. Epidemiol. 37, 698–701.

Gürtler, R.E., Ceballos, L.A., Ordóñez-Krasnowski, P., Lanati, L.A., Stariolo, R., Kitron, U., 2009. Strong host-feeding preferences of the vector Triatoma infestans modified by vector density: implications for the epidemiology of Chagas disease. PLoS Negl. Trop. Dis. 3, e447.

Guzman-Tapia, Y., Ramirez-Sierra, M.J., Escobedo-Ortegon, J., Dumonteil, E., 2005. Effect of Hurricane Isidore on *Triatoma dimidiata* distribution and Chagas disease transmission risk in the Yucatan Peninsula of Mexico. Am. J. Trop. Med. Hyg. 73, 1019–1025.

Hashimoto, K., Schofield, C.J., 2012. Elimination of *Rhodnius prolixus* in Central America. Parasit Vectors 5, 45.

Kot, M., Schaffer, W.M., 1986. Discrete-time growth-dispersal models. Math. Biosci. 80, 109–136.

Kot, M., Neubert, M., 2008. Saddle-point approximations, integrodifference equations, and invasions. Bull. Math. Biol. 70, 1790–1826.

Lehane, M., McEwen, P., Whitaker, C., Schofield, C., 1992. The role of temperature and nutritional status in flight initiation by Triatoma infestans. Acta Trop. 52, 27–38.

Li, B., Weinberger, H.F., Lewis, M.A., 2005. Spreading speeds as slowest wave speeds for cooperative systems. Math. Biosci. 196, 82–98.

Lui, R., 1989. Biological growth and spread modeled by systems of recursions. I. Mathematical theory. Math. Biosci. 93, 269–295.

Mac Cord, J.R., d'Almeida, S.C.G.R., 1986. The influence of temperature on the behaviour of *Triatoma infestans* (Klug, 1834) (Hemiptera, Reduviidae) under laboratory conditions: dispersion. Mem. Inst. Oswaldo Cruz 81, 162.

Magnus, W.O., Oberhettinger, F., Soni, R.P., 1966. Formulas and Theorems for the Special Functions of Mathematical Physics. Springer-Verlag, New York.

Medlock, J., Kot, M., 2003. Spreading disease: integro-differential equations old and new. Math. Biosci. 184, 201–222.

Menu, F., Ginoux, M., Rajon, E., Lazzari, C.R., Rabinovich, J.E., 2010. Adaptive developmental delay in Chagas disease vectors: an evolutionary ecology approach. PLoS Negl. Trop. Dis. 4, e691.

Miles, M.A., 1976. A simple method of tracking mammals and locating triatomine vectors of *Trypanosoma cruzi* in Amazonian forest. Am. J. Trop. Med. Hyg. 25, 671–674.

Minoli, S.A., Lazzari, C.R., 2006. Take-off activity and orientation of triatomines (Heteroptera: Reduviidae) in relation to the presence of artificial lights. Acta Trop. 97, 324–330.

Mollison, D., 1977. Spatial contact models for ecological and epidemic spread. J. R. Stat. Soc., 283–326.

Mollison, D., 1991. Dependence of epidemic and population velocities on basic parameters. Math. Biosci. 107, 255–287.

Murray, J.D., 1984. Asymptotic Analysis. Springer-Verlag, New York.

Naiff, M., Naiff, R.D., Barrett, T.V., 1998. Vetores selváticos de doença de Chagas na área urbana de Manaus (AM): atividade de vôo nas estações secas e chuvosas. Rev. Soc. Bras. Med. Trop. 31, 103–105.

Neubert, M.G., Caswell, H., 2000. Demography and dispersal: calculation and sensitivity analysis of invasion speed for structured populations. Ecology 81, 1613–1628.

Neubert, M.G., Kot, M., Lewis, M.A., 2000. Invasion speeds in fluctuating environments. Proc. R. Soc. Lond. Ser. B: Biol. Sci. 267, 1603–1610.

Nocerino, F., 1975. Insecticide susceptibility of *Rhodnius prolixus* and *Triatoma maculata* in Venezuela. VBC 75, 565.

Nouvellet, P., Dumonteil, E., Gourbière, S., 2013. The improbable transmission of Trypanosoma cruzi to human: the missing link in the dynamics and control of Chagas disease. PLoS Negl. Trop. Dis. 7, e2505.

Nouvellet, P., Cucunubá, Z.M., Gourbière, S., 2015. Chapter four - ecology, evolution and control of chagas disease: a century of neglected modelling and a promising future. In: Roy, M.A., Maria Gloria, B. (Eds.), Advances in Parasitology, Vol. 87. Academic Press, pp. 135–191.

Nouvellet, P., Ramirez-Sierra, M.J., Dumonteil, E., Gourbière, S., 2011. Effects of genetic factors and infection status on wing morphology of *Triatoma dimidiata* species complex in the Yucatan peninsula, Mexico. Infect. Genet. Evol. 11, 1243–1249.

Pacheco-Tucuch, F.S., Ramirez-Sierra, M.J., Gourbière, S., Dumonteil, E., 2012. Public street lights increase house infestation by the Chagas disease vector *Triatoma dimidiata*. PLoS One 7, e36207.

Patterson, J., Schwarz, M., 1977. Chemical structure, juvenile hormone activity and persistence within the insect of juvenile hormone mimics for *Rhodnius prolixus*. J. Insect Physiol. 23, 121–129.

Payet, V., Ramirez-Sierra, M., Rabinovich, J., Menu, F., Dumonteil, E., 2009. Variations in sex ratio, feeding, and fecundity of *Triatoma dimidiata* (Hemiptera: Reduviidae) among habitats in the Yucatan Peninsula, Mexico. Vector-Borne Zoonotic Dis. 9, 243–251.

Pelosse, P., Kribs-Zaleta, C.M., Ginoux, M., Rabinovich, J.E., Gourbiere, S., Menu, F., 2013. Influence of vectors' risk-spreading strategies and environmental stochasticity on the epidemiology and evolution of vector-borne diseases: the example of Chagas' disease. PLoS One 8, e70830.

Petrovskii, S.V., Li, B.-L., 2006. Exactly Solvable Models of Biological Invasion. Chapman and Hall, CRC Press, Boca Raton.

Pinto Dias, J.C., 2013. Human Chagas disease and migration in the context of globalization: some particular aspects. J. Trop. Med. 2013, 9.

Powell, J.A., Slapničar, I., van der Werf, W., 2005. Epidemic spread of a lesion-forming plant pathogen—analysis of a mechanistic model with infinite age structure. Linear Algebra Appl. 398, 117–140.

Radcliffe, J., Rass, L., 1984. Saddle point approximations in n-type epidemics and contact birth processes. Rocky Mt. J. Math. 14, 599–618.

Radcliffe, J., Rass, L., 1997. Discrete time spatial models arising in genetics, evolutionary game theory, and branching processes. Math. Biosci. 140, 101–129.

Rascalou, G., Pontier, D., Menu, F., Gourbière, S., 2012. Emergence and prevalence of human vector-borne diseases in sink vector populations. PLoS One 7, e36858.

Scaraffia, P.Y., Gerez De Burgos, N.M., 2000. Effects of temperature and pH on hexokinase from the flight muscles of Dipetalogaster maximus (Hemiptera: Reduviidae). J. Med. Entomol. 37, 689–694.

Schofield, C., 1985. Control of Chagas' disease vectors. Br. Med. Bull. 41, 187–194.

Schofield, C., Lehane, M., McEwan, P., Catalá, S., Gorla, D., 1991. Dispersive flight by *Triatoma sordida*. Trans. R. Soc. Trop. Med. Hyg. 85, 676–678.

Schofield, C.J., Lehane, M.J., McEwen, P., Catala, S.S., Gorla, D.E., 1992. Dispersive flight by *Triatoma infestans* under natural climatic conditions in Argentina. Med. Vet. Entomol. 6, 51–56.

Schreiber, S., Ryan, M., 2011. Invasion speeds for structured populations in fluctuating environments. Theor. Ecol. 4, 423–434.

Shigesada, N., Kawasaki, K., 2002. Invasion and the range expansion of species: effects of long-distance dispersal. Dispersal Ecol., 350–373.

Sjogren, R.D., Ryckman, R.E., 1966. Epizootiology of *Trypanosoma cruzi* in Southwestern North America VIII. Nocturnal Flights of *Triatoma protracta* (Uhler) as Indicated by collections at black light traps. J. Med. Entomol. 3, 81–92.

Skellam, J.G., 1951. Random dispersal in theoretical populations. Biometrika, 196–218.

Slimi, R., El Yacoubi, S., Dumonteil, E., Gourbiere, S., 2009. A cellular automata model for Chagas disease. Appl. Math. Model. 33, 1072–1085.

Szegö, G., 1975. Orthogonal Polynomials. American Mathematical Society (Colloquium Publications), p. 23, Providence.

Tanowitz, H.B., Weiss, L.M., Montgomery, S.P., 2011. Chagas disease has now gone global. PLoS Negl. Trop. Dis. 5, e1136.

Tonn, R., Carcavallo, R., Ortega, R., Carrasquero, B., 1976. Methods of studying Triatominae in a sylvatic environment. Bole. de la Dir. de Malariol. y Saneam. Ambient. 16, 146–152.

Van Assche, W., 1987. Asymptotics for Orthogonal Polynomials (Lecture Notes in Math 1265). Springer, Berlin.

Vazquez Prokopec, G., Ceballos, L., Marcet, P., Cecere, M., Cardinal, M., Kitron, U., Gürtler, R., 2006. Seasonal variations in active dispersal of natural populations of Triatoma infestans in rural north-western Argentina. Med. Vet. Entomol. 20, 273–279.

Waleckx, E., Gourbière, S., Dumonteil, E., 2015a. Intrusive versus domiciliated triatomines and the challenge of adapting vector control practices against Chagas disease. Mem. Inst. Oswaldo Cruz 110, 1–15.

Waleckx, E., Camara-Mejia, J., Ramirez-Sierra, M.J., Cruz-Chan, V., Rosado-Vallado, M., Vazquez-Narvaez, S., Najera-Vazquez, R., Gourbière, S., Dumonteil, E., 2015b. An innovative ecohealth intervention for Chagas disease vector control in Yucatan, Mexico. Trans. R. Soc. Trop. Med. Hyg. 109, 143–149.

Weinberger, H.F., 1982. Long-time behavior of a class of biological models. SIAM J. Math. Anal. 13, 353–396.

Weinberger, H.F., 2002. On spreading speeds and traveling waves for growth and migration models in a periodic habitat. J. Math. Biol. 45, 511–548.

Weinberger, H.F., Lewis, M.A., Li, B., 2002. Analysis of linear determinacy for spread in cooperative models. J. Math. Biol. 45, 183–218.

WHO, 2010. Weekly Epidemiological Record, 85, pp. 329–336.

Wisnivesky Colli, C., Gürtler, R.E., Solarz, N.D., Schweigmann, N.J., Pietrokovsky, S. M., Alberti, A., Flo, J., 1993. Dispersive flight and house invasion by Triatoma guasayana and Triatoma sordida in Argentina. Mem. Inst. Oswaldo Cruz 88, 27–32.

Wood, S.F., 1967. Ecological Relationships of Triatoma p. *protacta* (Uhler) in Griffith Park, Los Angeles, Calif. Pacific Insects 9, 537–550.

Yong, K.E., Mubayi, A., Kribs, C.M., 2015. Agent-based mathematical modeling as a tool for estimating Trypanosoma cruzi vector–host contact rates. Acta Trop. 151, 21–31.

Zeledón, R., 1975. Effects of triatomine behavior on Trypanosoma transmission. PAHO Sci. Publ. 318, 326–329.

Zeledón, R., 1981. El *Triatoma dimidiata* [Latreille, 1811] y su Relación con la Enfermedad de Chagas. Editorial Universidad Estatal a Distancia, San José, Costa Rica, p. 146.

Zeledón, R., Guardia, V.M., Zuñiga, A., Swartzwelder, J.C., 1970. Biology and ethology of *Triatoma dimidiata* (Latreille, 1811) II. Life span of adults and fecundity and fertility of females. J. Med. Entomol. 7, 462–469.